Event Identification From PMT Hit Patterns

SNO-STR-94-044

I. Blevis 9/94

W O R K I N P R O G R E S S

Abstract

Using seven analyses (variables) related to the compactness, or to the cherenkov ring structure of SNO events, separation of cc and nc events in 1 years (Queens) monte carlo data has been realized at the .5 to 1.1 sigma level, and in the less than 80 PMT hits per event range. Cooresponding enriched nc data sets can then be realized. The most promising analyses show pathological component behavior that could be improved to yield still higher separations. The independence of the analyses is not yet utilized and is also expected to increase the separation.

Purpose:

To find variables in which cc, nc and background events have separated distinguishable distributions, thereby allowing a probabilistic event by event computer aided identification.

Motivation:

1. separate location and direction of 2 electron (nc) events
2. correlation of multiple scattered track segments of single electron (cc) events.

The Moliere multiple scattering cross section (DIXIT 81) was used to estimate the probability of seeing 2 rings in a SNO event. The distributions for 5 and 10 MeV electrons and various path path lengths of H2O up to the electron range are show in fig 1 . It is seen that there is substantial probability of finding the electron travelling at more than 20 degrees from its original path in less than half of its range. The full range of a 10 MeV e- in H2O is about 4 cm.

Thus, one or two close rings may be expected from cc events in SNO. On the other hand, nc events of the same number of pmt hits are likely to have originated with more than one electron, each with lower energy and so are less likely to produce one or two easily identifiable and correlated Cherenkov rings.

After producing an event display that removed geometrical projection effects from the data, visual inspection showed that Cherenkov rings were often to be found with +-10 degrees scatter from the expected opening angle of 41 degrees. This range is compatible with the mean multiple scattering angles seen for smaller frations of the electron range from the figure.

Method:

A reference frame was chosen that suitably located, oriented, and scaled the PMT hit pattern of a QMC monte-carlo generated SNO event. The frame consisted of spherical coordinates with origin at the vertex returned by the QMC event fitter and polar axis extending towards the center of mass (on the spherical shell of the PSUP) of the hit pmts. With the detector geometry removed in this way, parameters were defined and histogramed for QMC cc and nc data sets (1000 events each). The first variable was the average polar angle of the hit pmts of the event. The second variable was the width of the polar angle distribution for each event. The third was the connectivity as defined by the average nearest neighbor angular distance of the pmts of the event.

Furthermore, an event display was developed to show the event in this aspect. Cherenkov rings were evident in this view as expected and a ring finder algorithm was written. It works by scanning the space in the neighborhood of the polar axis (defined above) and counting the number of hit pmts that are within 10 degrees of the cherenkov angle from the test point. The point with the highest count is chosen as a ring center. The significance of a found ring is indicated by the distribution of used pmt hits (upper right corner of display). A search for a second ring is made with the unused pmt hits. The percentage use of the PMT's in the rings (ie the success at matching the expected cc characteristics) as well as the angle between found rings was histogramed. This analysis is just beginning.

Results:
---

variable 1; theav: fig 2.

Average PMT polar angle with respect to the PMT center of mass in the vertex centered frame;

The cc distribution shows a peak at 44 degrees and another suggestion of one at 50. The first one is probably single cherenkov rings, and the second one can be studied and probably identified by the event display. The nc distribution is flatter and shifted. The peak separation is .55 sigma where sigma is the combination in quadrature of the two peak sigmas. Using calibration data from the running SNO the component distributions in mixed data sets of various ratios cc/nc = (1:1) to (3:1) can be identified at the percent level in one year's statistics. The distributions show a relatively clean nc sample available at high values of the variable. As well, since this variable is shown to be energy independent (fig 4), separate cc and nc spectra would be possible. The possibility is that these distributions will further improve by the improvement in the choice of the polar axis in the choice of the coordinate system.

variable 2; thesig: fig 3.

Width of PMT polar angle distribution per event;

This variable shows less shape differences, but improved separation of the centers for cc and nc, .83 sigma . Thus though the distributions are more closely each a single Gaussian, the mixed distribution (fig 3.b) is not. This is another opportunity to 'discover' both cc and nc in the data. As well, the same possibilities with calibration data exist as described above.

The correlation of these distributions with variable 1 is not perfect (fig 5) and thus there is perhaps some gain to be realized from a combined variable.

variable 3; connectivity: fig 6.

The mean nearest neighbor angular distance per event; Though the peak separation is only .48 sigma the peaks show non-random structure that may be further understood. The variable is energy independent. As well this variable is not correlated with the previous one offering another opportunity to combine.

variable 4; angle ring1 axis to ring2 axis. fig 7.

The event display in figure seven show the pmts hits on a polar plot (never mind the cartesian axes) centered on the line from the QMC fitted vertex to the hit PMT center of mass (in theta,phi space). Two rings are evident and helped in identification by the offcenter projection of the anuli in the display. The upper right corner illustrates that the position of the anulus of ring 1 acutely maximizes the number of contained pmt hits. The upper left corner chos that a (loose) time cut of -3 to 6 ns from the expected time of arrival given the QMC fitter vertex has been applied to eliminate large angle Raylaieh scattered photons. These two rings are almost 90 degrees apart ! and 89% of the PMT's have been used in the ring reconstruction. Though the difference between cc and nc is clear, fig 8 this variable is not the best.

Fig 9a-c shows more event examples.

variable 5; ring 1 hit pmt useage fig 10 (a-f).

figures 10 (a,b) show .75 sigma separation for the whole cc and nc data sets. Figures 10 (c,d) , and (e,f) show the energy slices of nPMThit<40, and 40<nPMThit<80 respectively. the separations are 1.0 and .80 sigma.

variable 6; ring 2 hit pmt useage fig 11 (a-f).

This variable is the ratio of hit pmts used in a second found ring of those that remain unused in ring 1, provided more than 5 remain. The separations of cc and cn are .74 , .89 , and .79 for the three nhit regions described above. A non physical double peak exist in the cc distributions that suggests that this result could be further improved.

variable 7; pmt useage in ring 1 or 2. fig 12(a-f):

The separations are .79, 1.1, and .9 . The nonphysical pathology remains to be improved.

variable 8; event compactness:

The number of hit PMTs that can be contianed in a given sector size, sutiable optimised around the PMT center of mass. Figures and discussion to be included.

All result are sumarized in table 1.

SNOMAN 2_05 / QMC : The nhit distributions for cc and nc from the two MC are included . fig 13. Substantial differences in number and shape are evident. These cc/nc studies commenced with SNOMAN 2_05 but were switched to QMC for comparisson with other methods.

Table 1 Summary of Performance of Variables.

\ Data Set: / variable: \	CC mean	CC sigma	NC mean	NC sigma	separation * (delta/sigma)
Theav	47.4	5.	52.6	7.9	5.2/9.4 = .55
Thesig	21.9	4.9	28.4	6.1	6.5/7.8 = .83
connectivity	.65	.15	.74	.15	.095/.20= .48
angle r1-r2	42	16	49	17	7/22 = .31
r1 pmt use	.53	.091	.44	.08	.09/.12 = .75
r2 pmt use	.53	.1	.43	.091	.1/.13 = .74
r1+r2 pmt use	.77	.075	.68	.086	.9/.11 = .79
cut: nhit<40 :					
r1 pmt use	.58	.11	.45	.08	.13/.13 = 1.0
r2 pmt use	.58	.13	.44	.09	.14/.16 = .89
r1+r2 pmt use	.81	.078	.69	.082	.12/.11 = 1.1
cut: 40<nhit<80 :					
r1 pmt use	.53	.081	.44	.081	.09/.11 = .80
r2 pmt use	.52	.091	.43	.091	.09/.13 = .70
r1+r2 pmt use	.77	.070	.67	.087	.10/.11 = .9

* separation measured in units of the combined sigmas:
sigma= sqrt(sigmaCC**2 + sigmaNC**2)

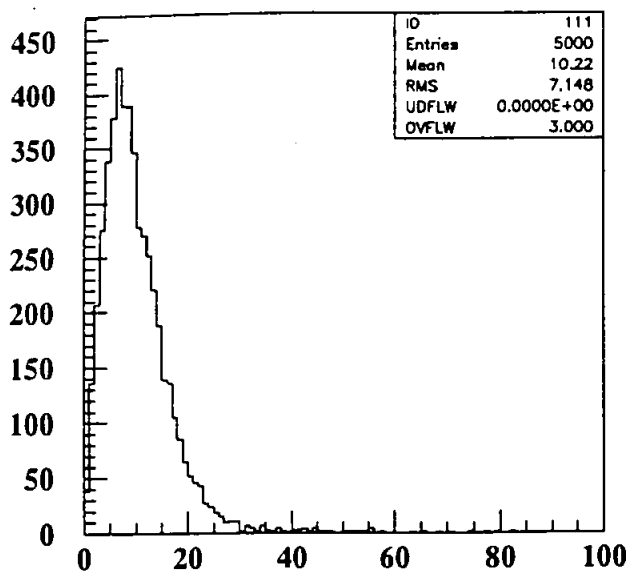

angle E=5MeV t=.1

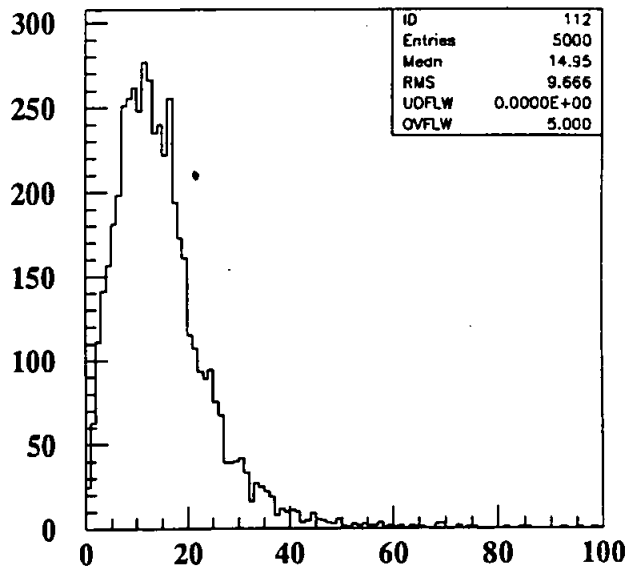

angle E=5MeV t=.2

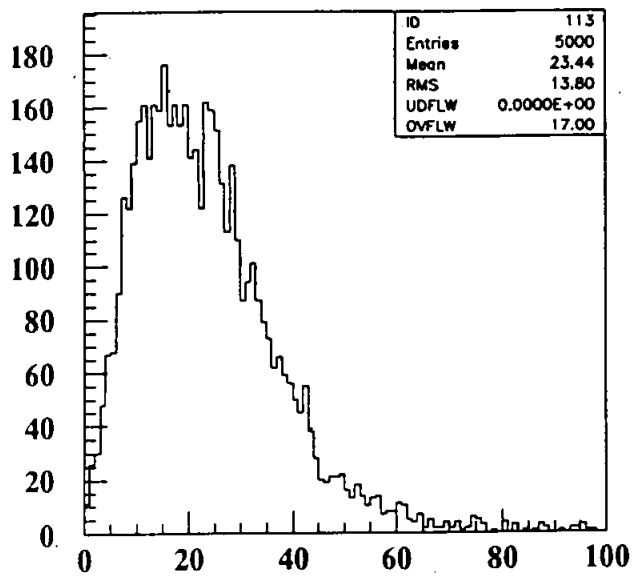

angle E=5MeV t=.5

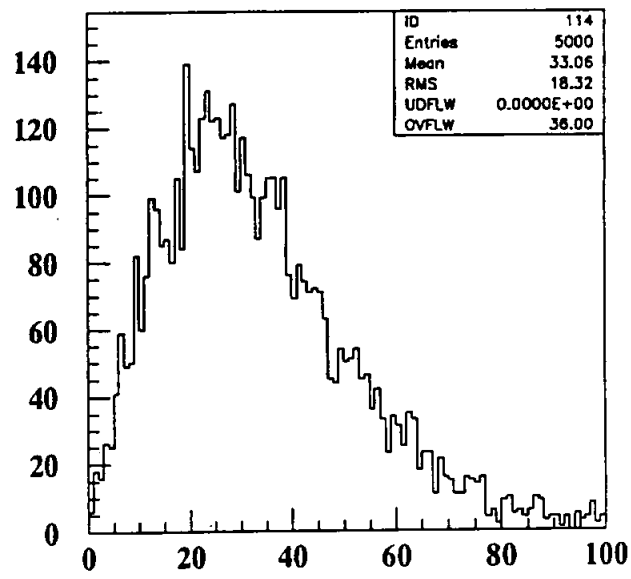

angle E=5MeV t=1.

fig 1a

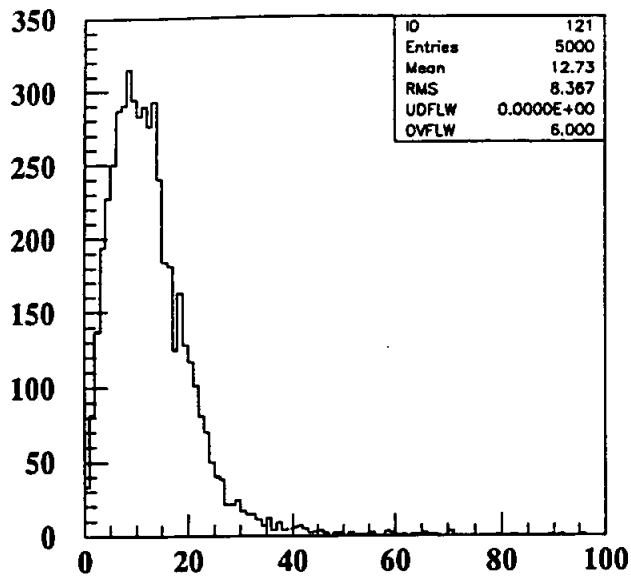

angle E=10MeV t=.5

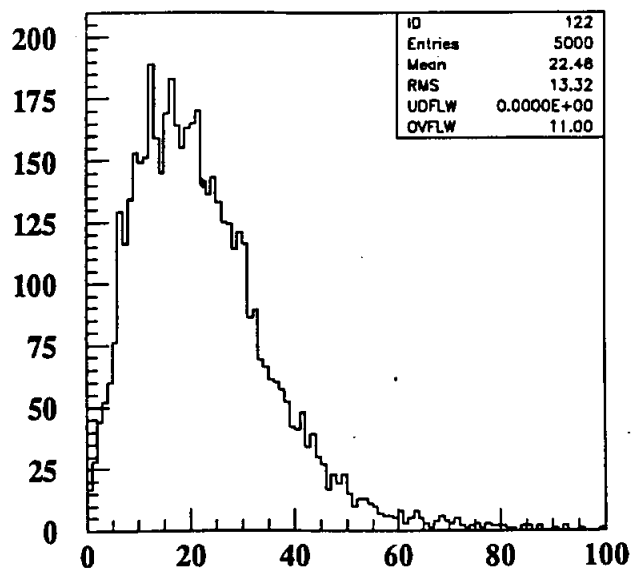

angle E=10MeV t=1.5

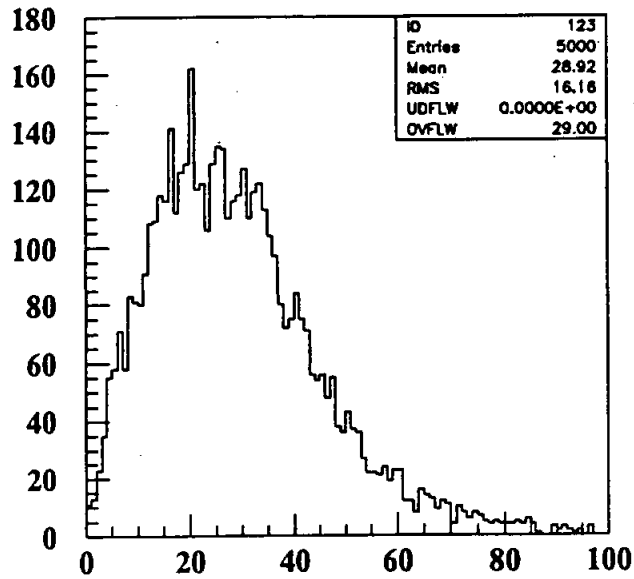

angle E=10MeV t=2.5

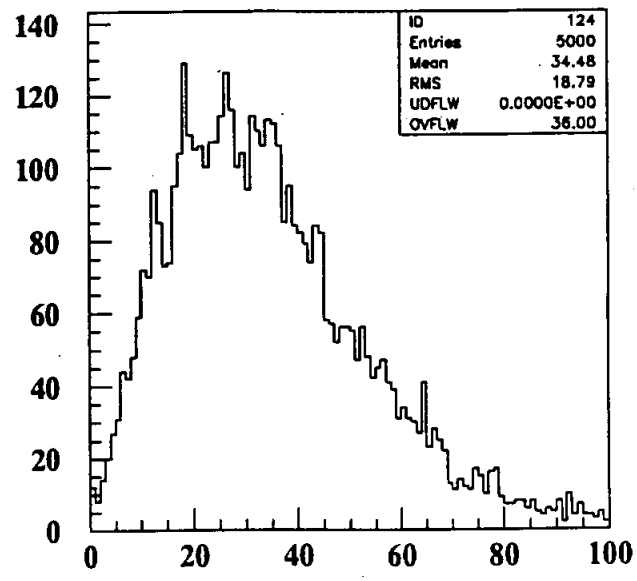

angle E=10MeV t=3.5

fig 16

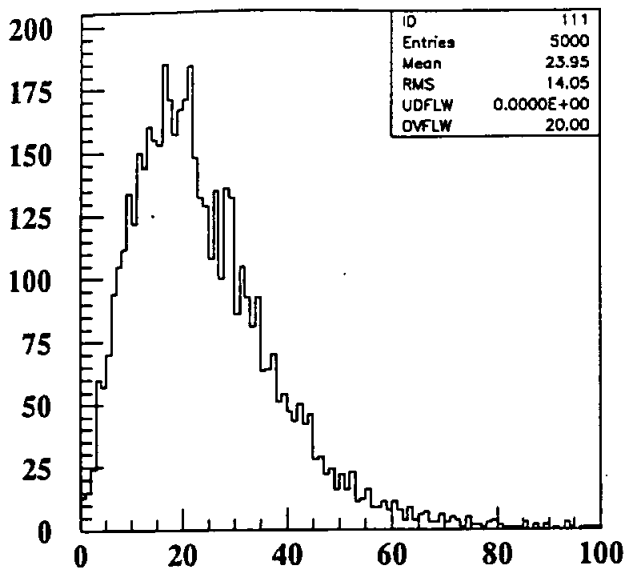

angle E=5MeV t=.5

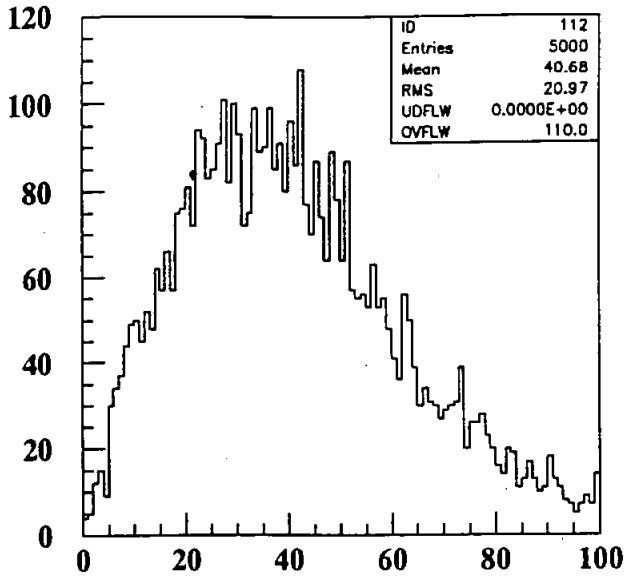

angle E=5MeV t=1.5

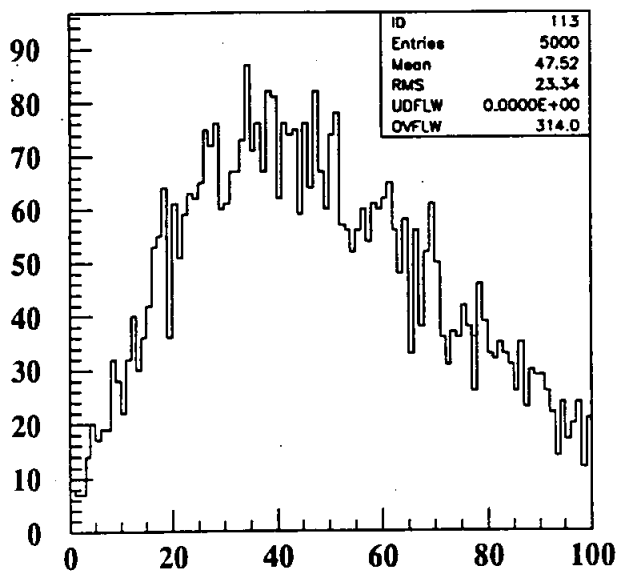

angle E=5MeV t=2.5

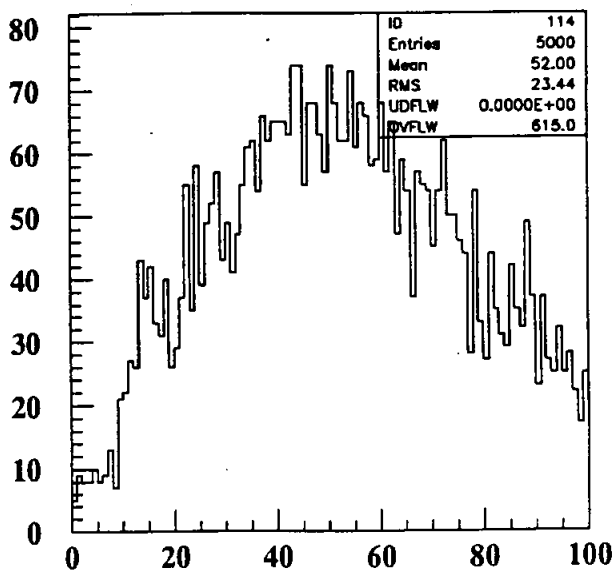

angle E=5MeV t=3.5

fig 1c

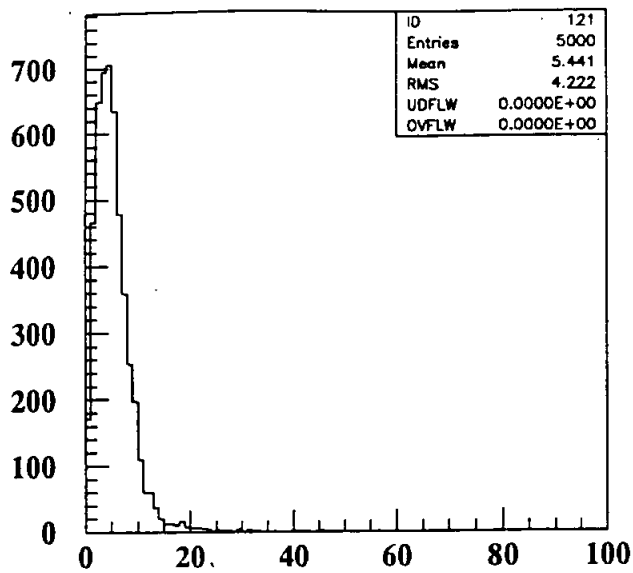

angle E=10MeV t=.1

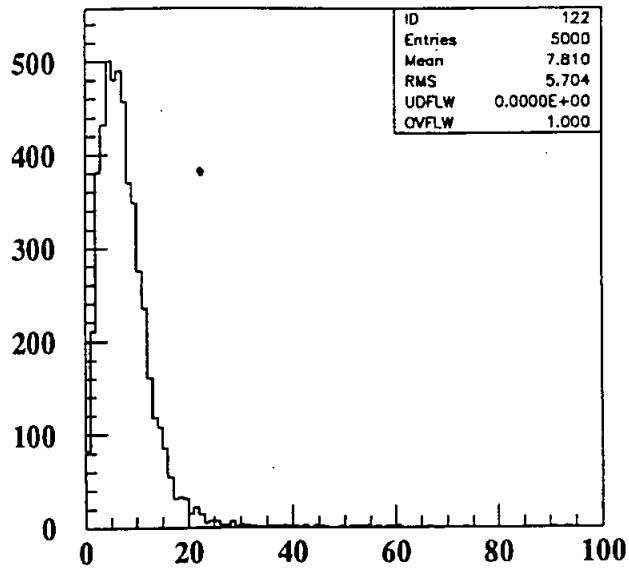

angle E=10MeV t=.2

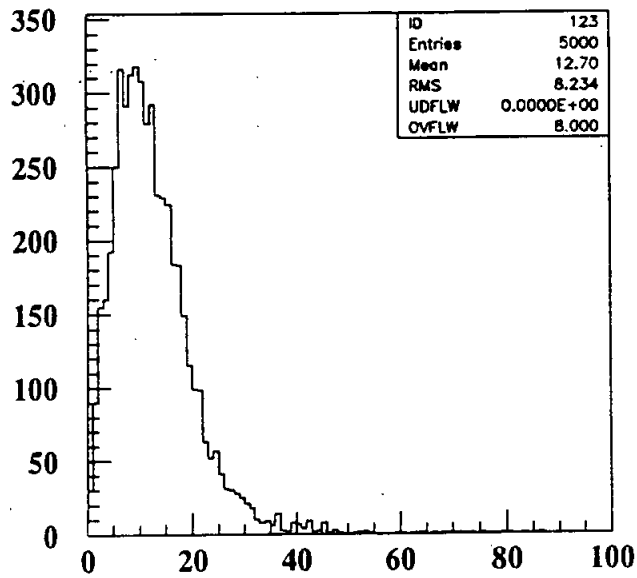

angle E=10MeV t=.5

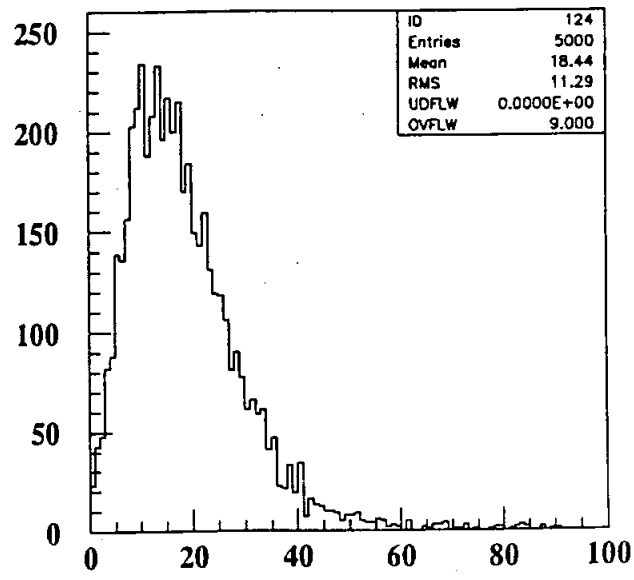

angle E=10MeV t=1.

fig 1d.

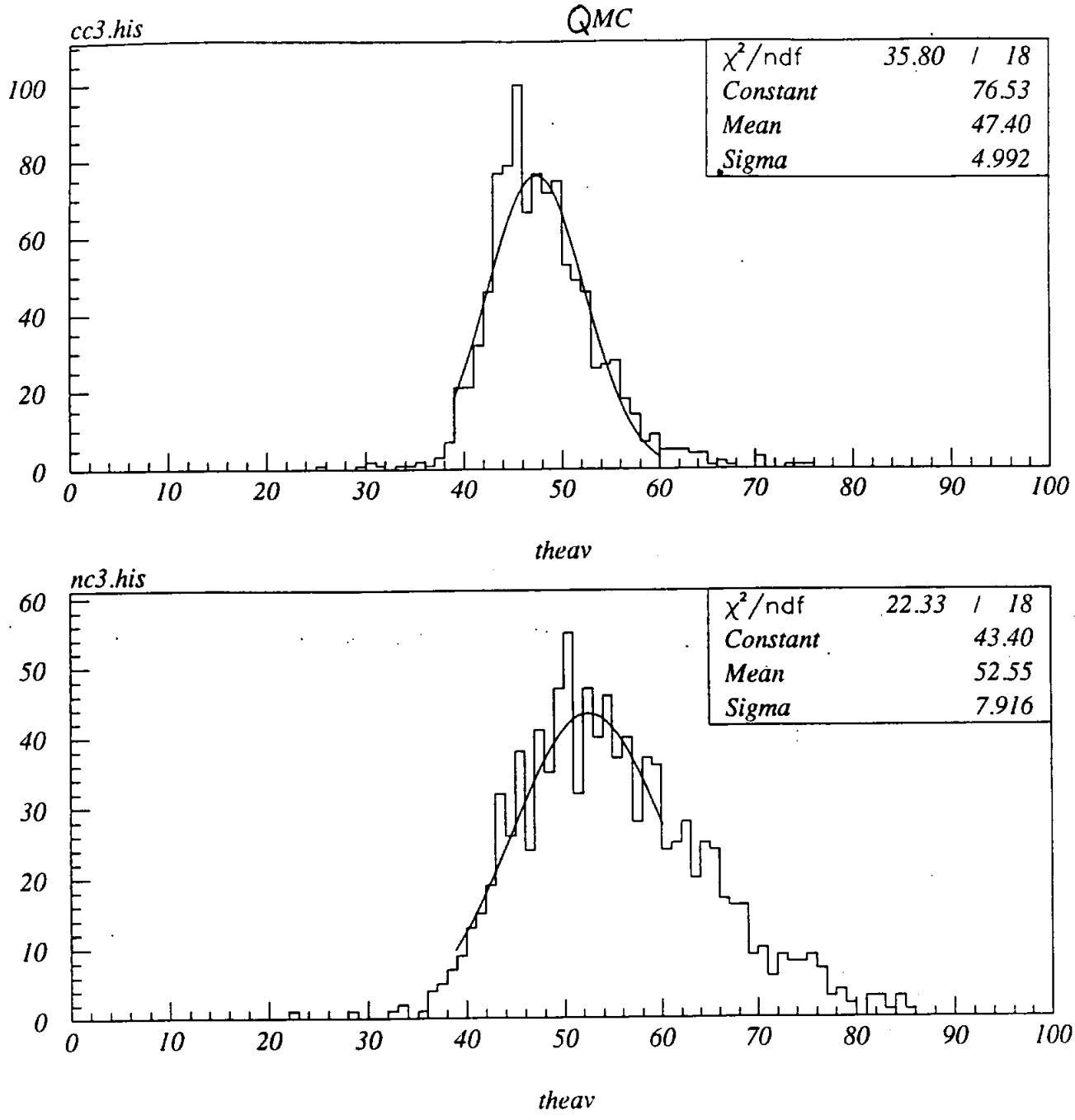
QMC
cc3.his
χ²/ndf 35.80 / 18
Constant 76.53
Mean 47.40
Sigma 4.992
theav
nc3.his
χ²/ndf 22.33 / 18
Constant 43.40
Mean 52.55
Sigma 7.916
theav

fig 2

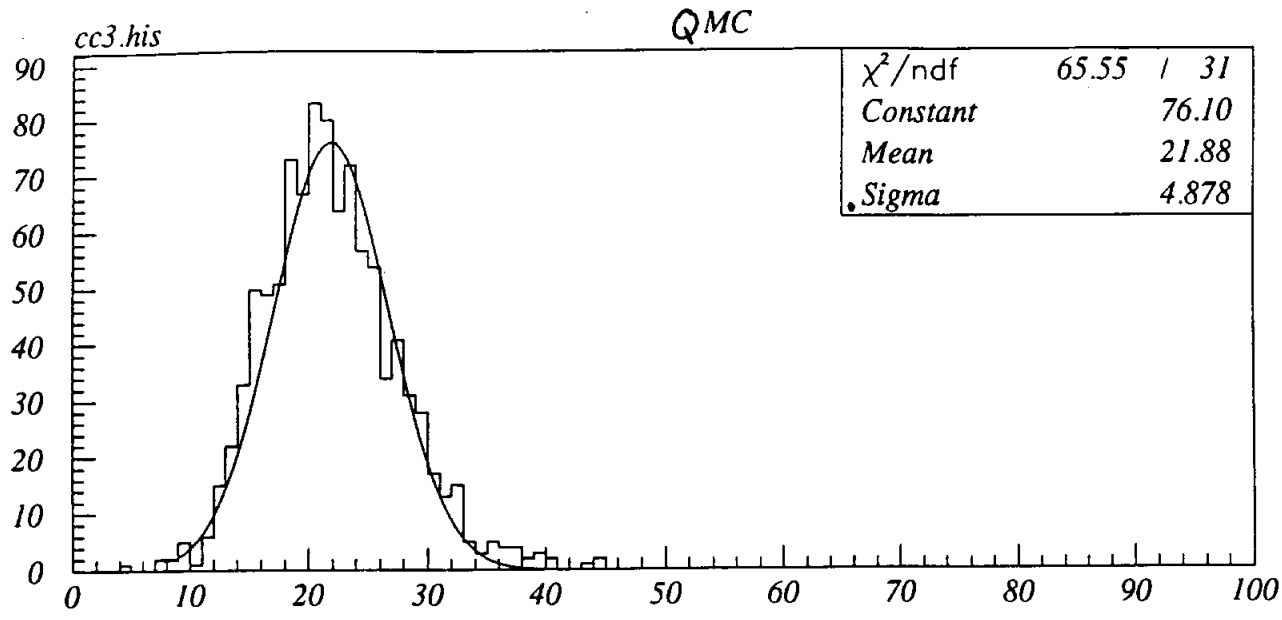
QMC
cc3.his
χ²/ndf 65.55 / 31
Constant 76.10
Mean 21.88
Sigma 4.878
thesig

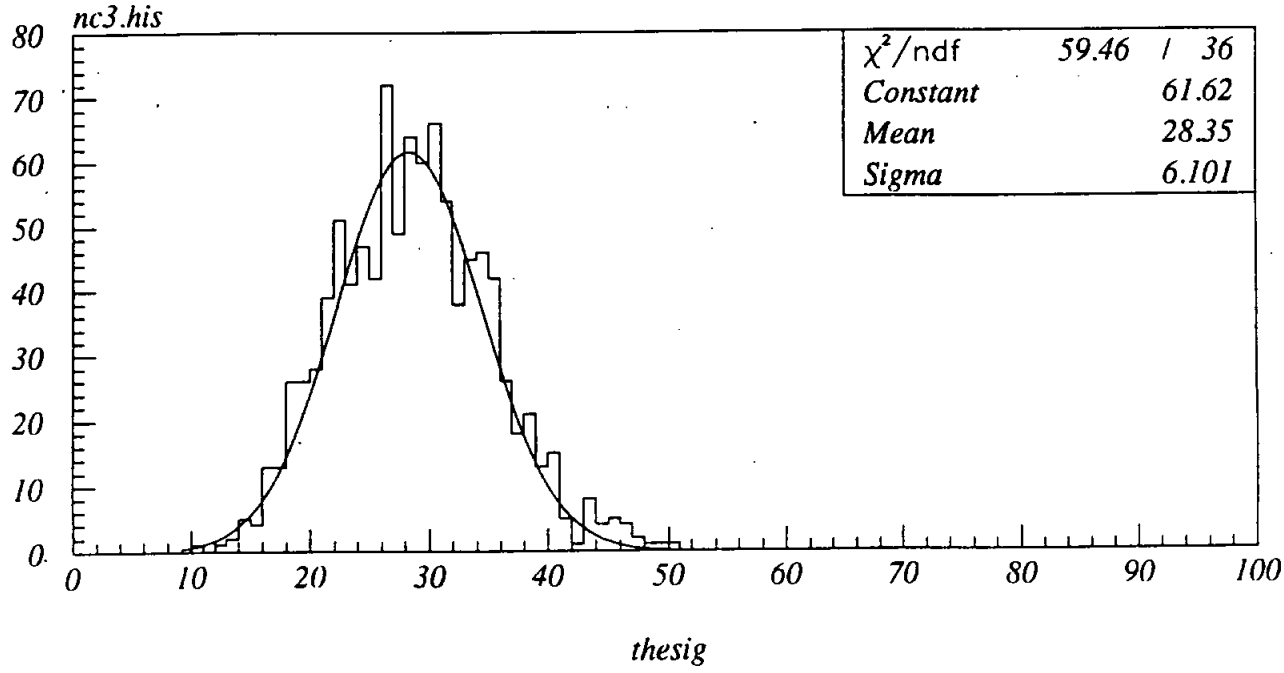
nc3.his
χ²/ndf 59.46 / 36
Constant 61.62
Mean 28.35
Sigma 6.101
thesig

fig 3

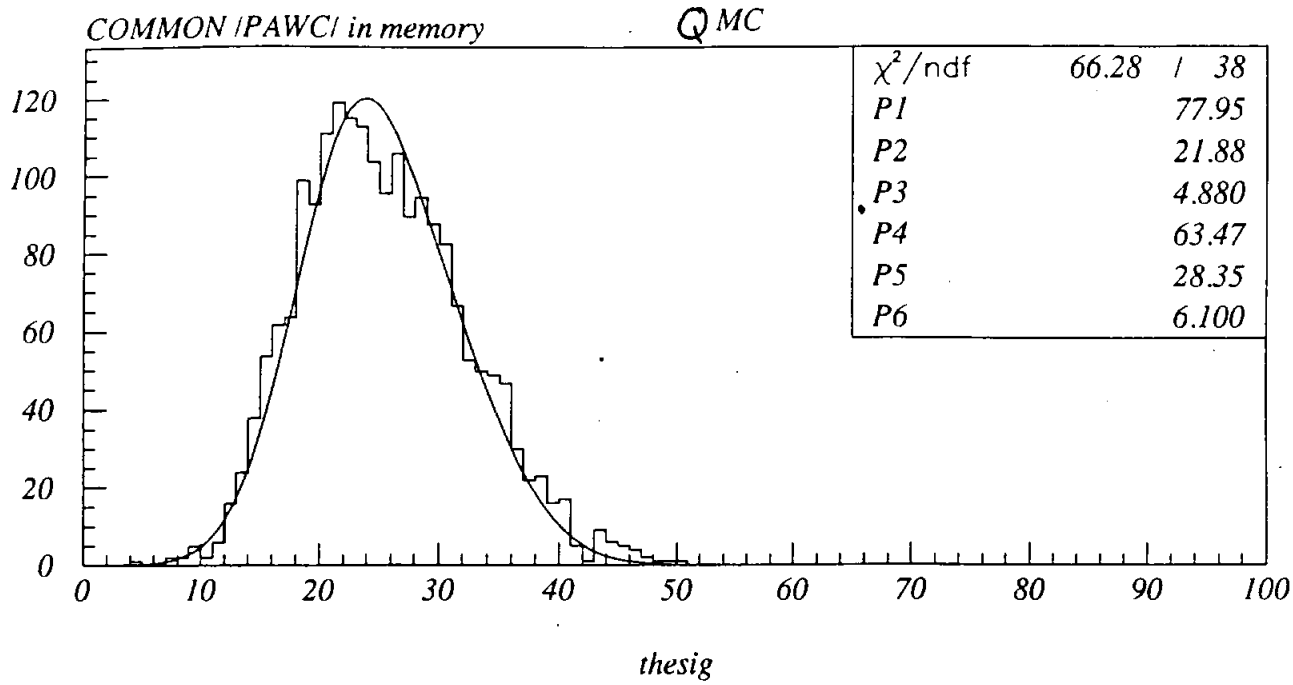
COMMON /PAWC/ in memory
Q MC
χ²/ndf 66.28 / 38
P1 77.95
P2 21.88
P3 4.880
P4 63.47
P5 28.35
P6 6.100
120
100
80
60
40
20
0
0 10 20 30 40 50 60 70 80 90 100
thesig

fig 3b

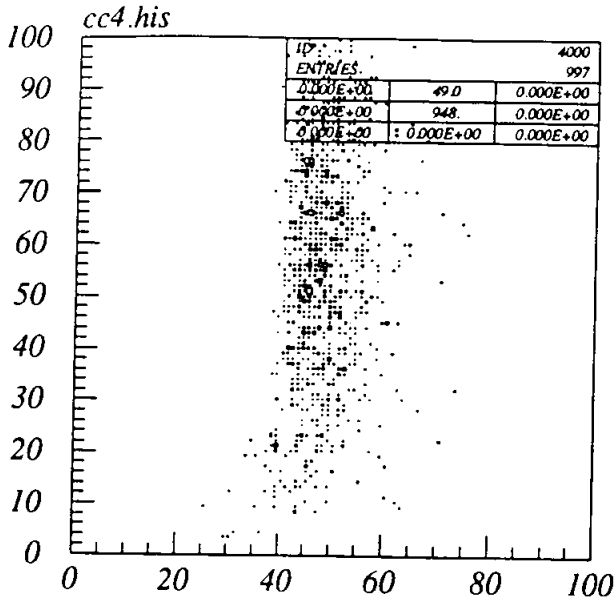

nhit vs theav

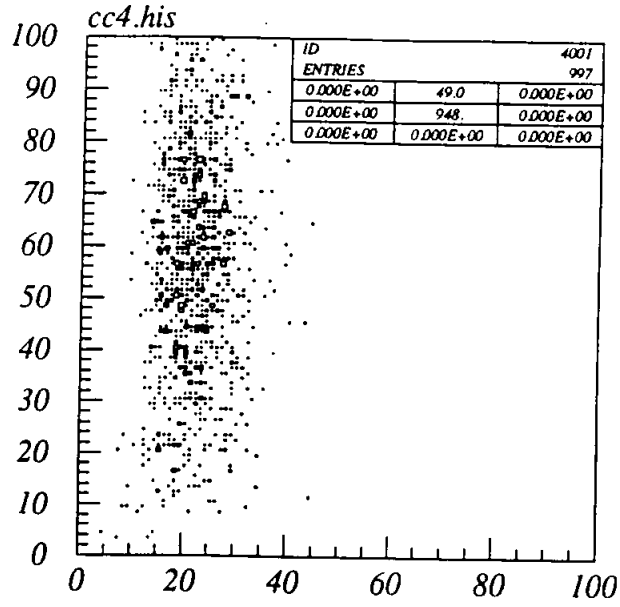

nhit vs thesig

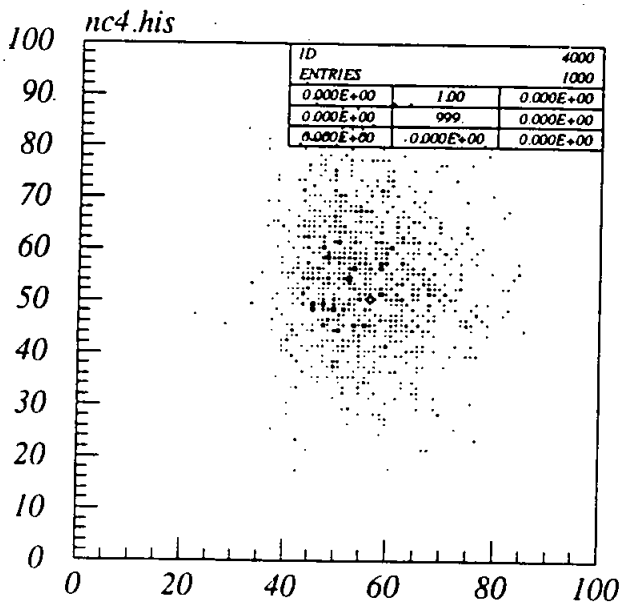

nhit vs theav

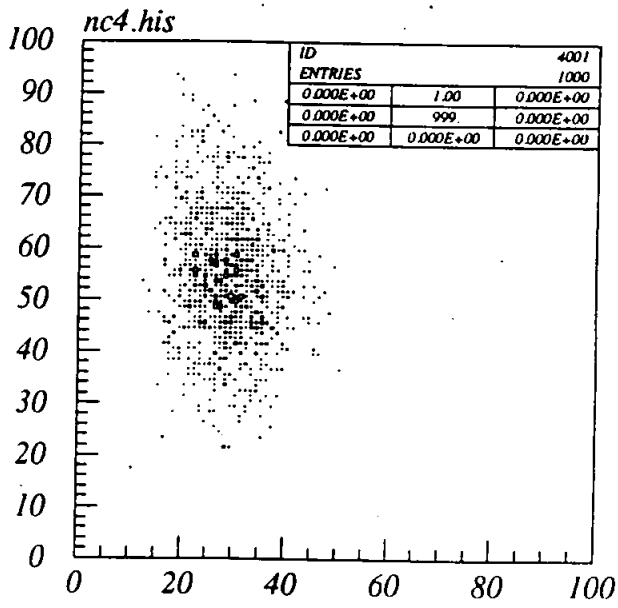

nhit vs thesig

fig 4

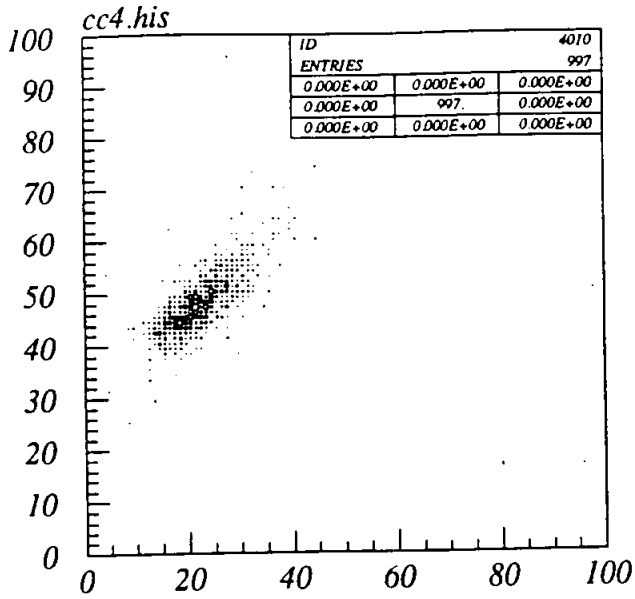

theav vs thesig

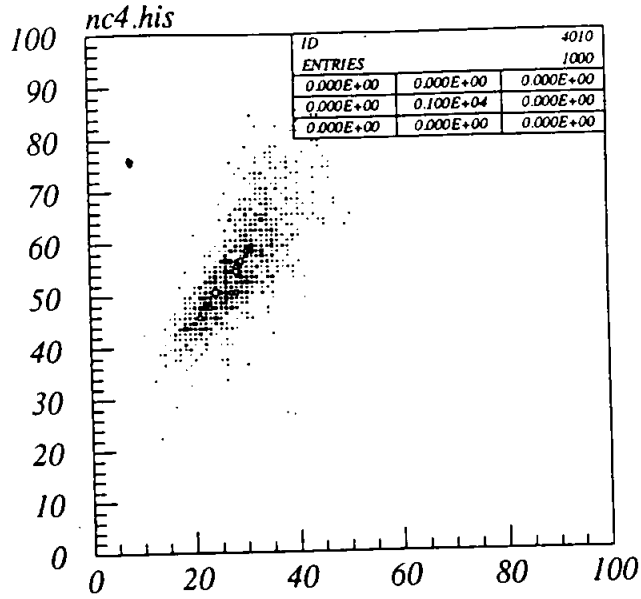

theav vs thesig

fig 5

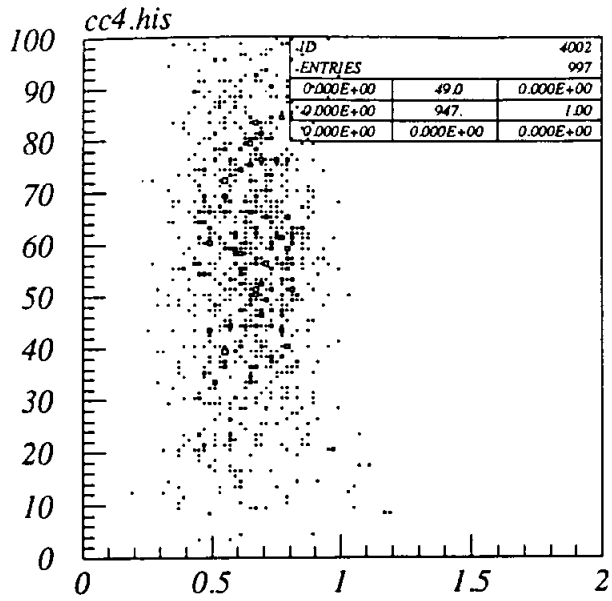

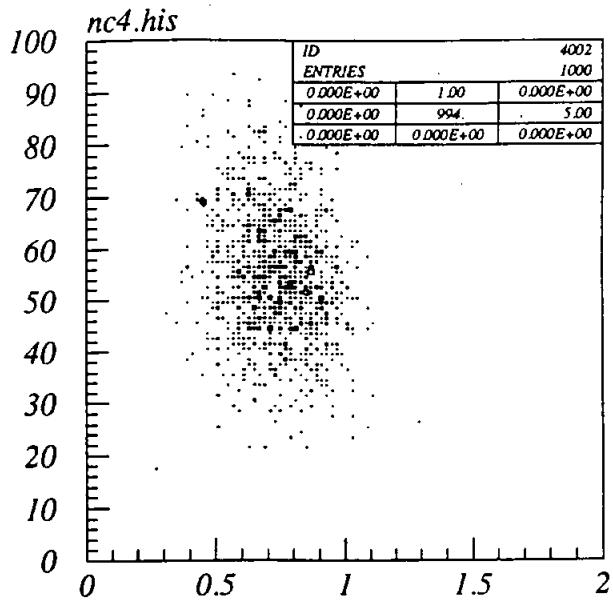

nhit vs connec

nhit vs connec

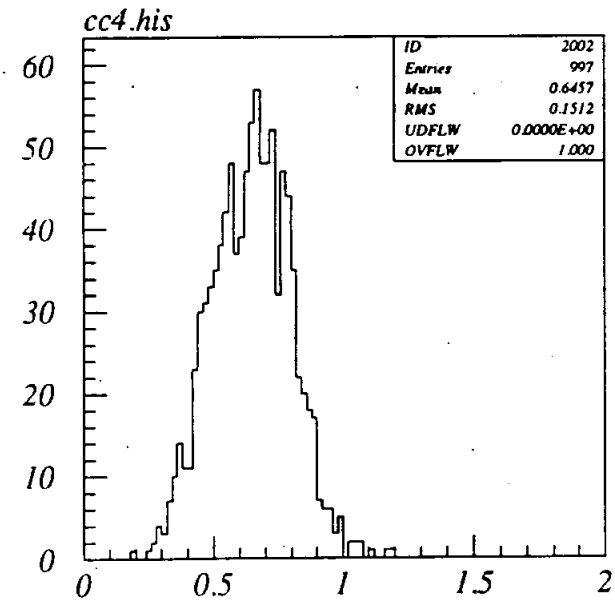

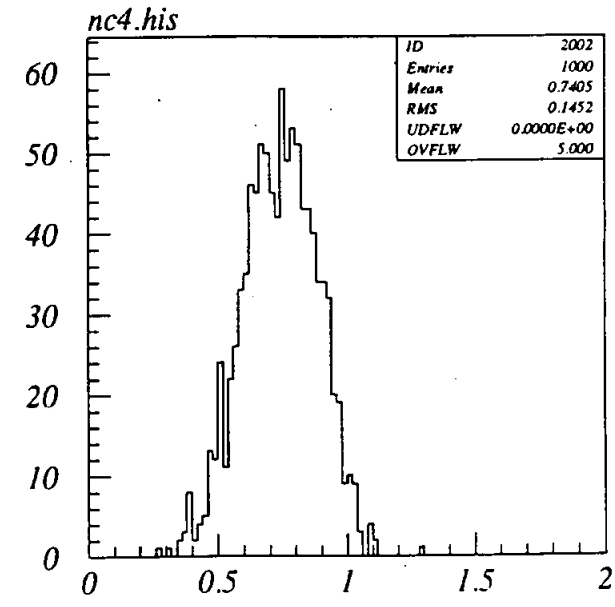

connectivity

connectivity

fig 6

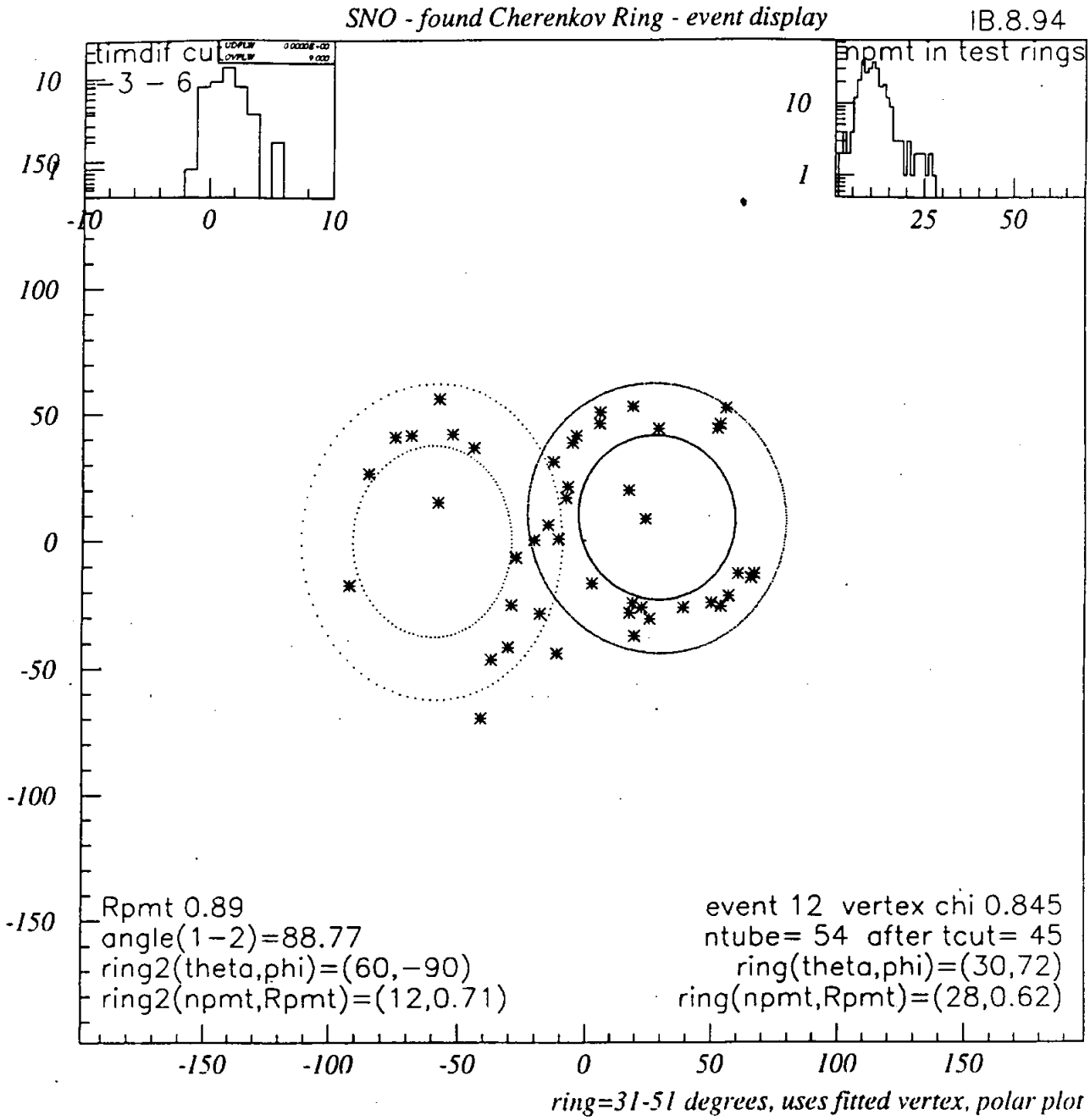
SNO - found Cherenkov Ring - event display
IB.8.94
timdif cut
-3 - 6
npmt in test rings
Rpmt 0.89
angle(1-2)=88.77
ring2(theta,phi)=(60,-90)
ring2(npmt,Rpmt)=(12,0.71)
event 12 vertex chi 0.845
ntube= 54 after tcut= 45
ring(theta,phi)=(30,72)
ring(npmt,Rpmt)=(28,0.62)
ring=31-51 degrees, uses fitted vertex, polar plot

fig 7

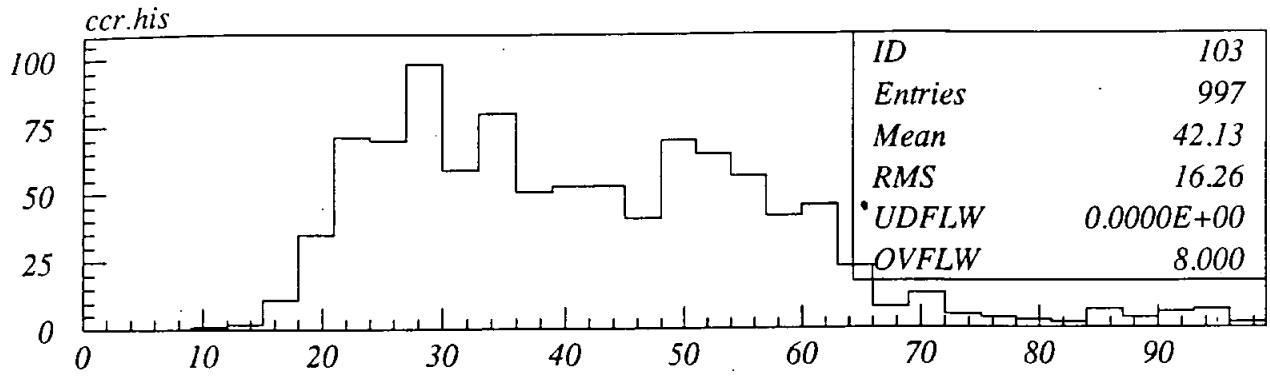

angle ring1-ring2

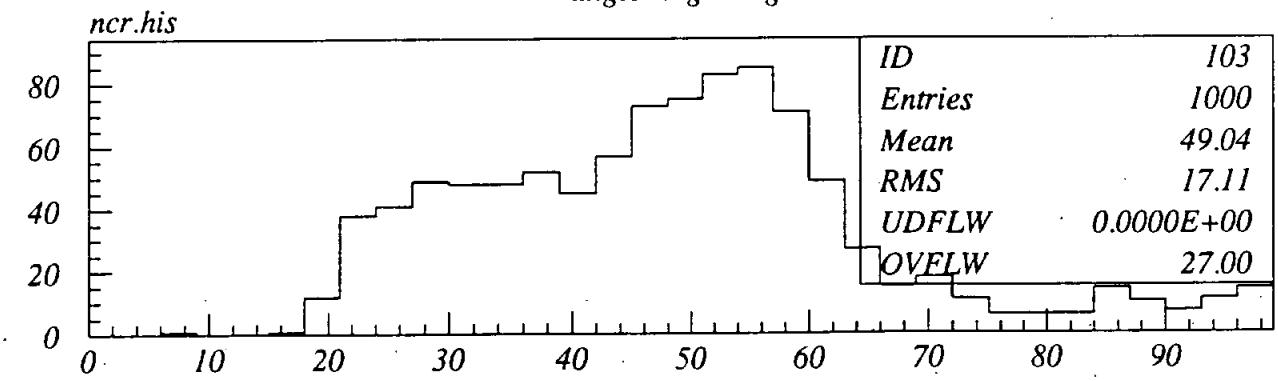

angle ring1-ring2

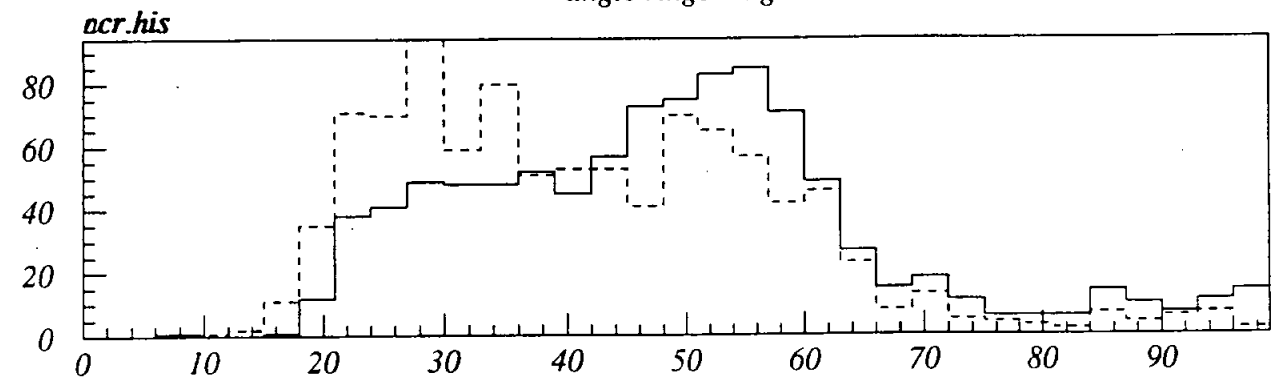

angle ring1-ring2

fig 8

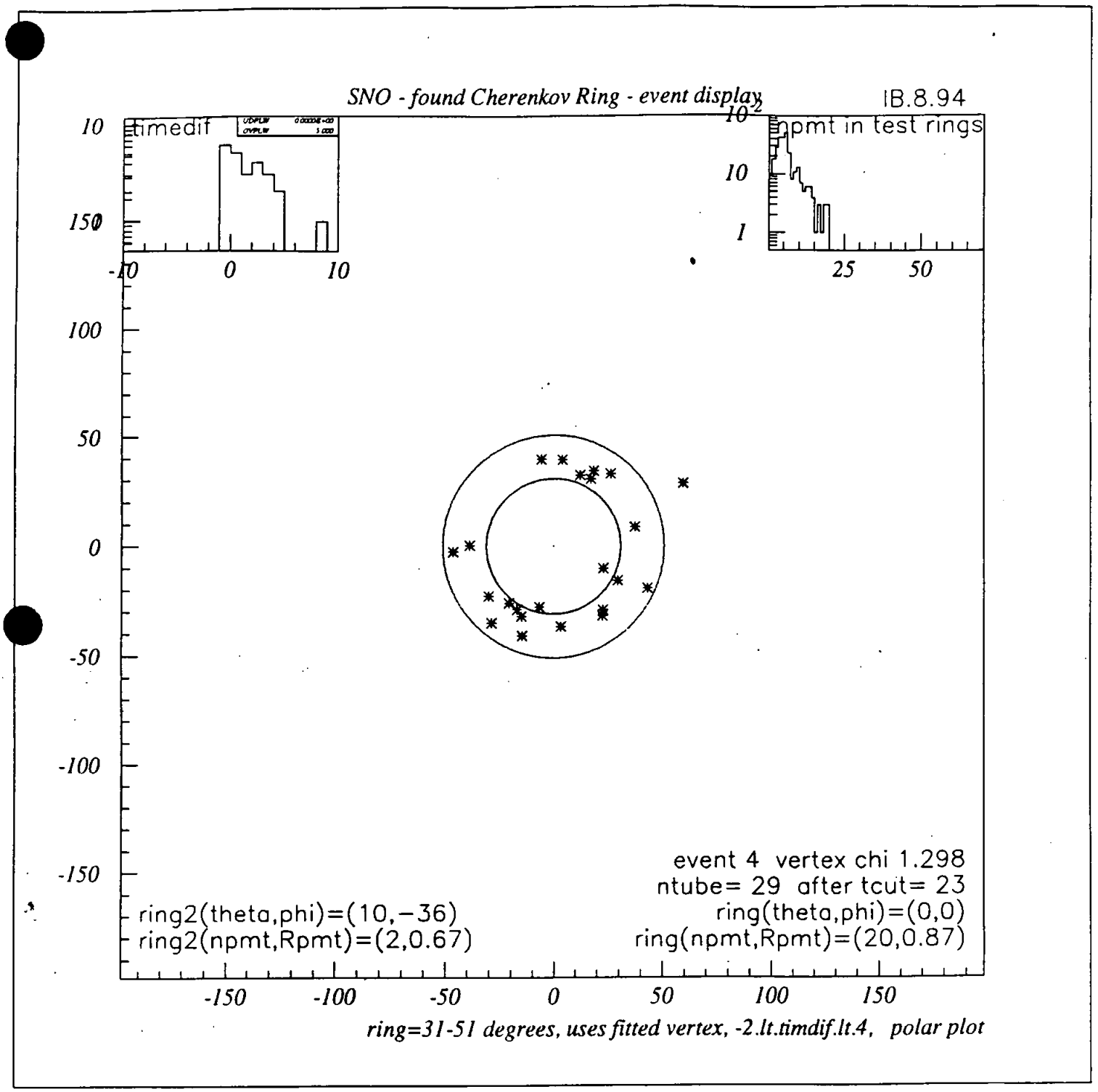
SNO - found Cherenkov Ring - event display
18.8.94
timedif
npmt in test rings
event 4 vertex chi 1.298
ntube= 29 after tcut= 23
ring(theta,phi)=(0,0)
ring(npmt,Rpmt)=(20,0.87)
ring2(theta,phi)=(10,−36)
ring2(npmt,Rpmt)=(2,0.67)
ring=31-51 degrees, uses fitted vertex, -2.lt.timdif.lt.4, polar plot

fig 9a

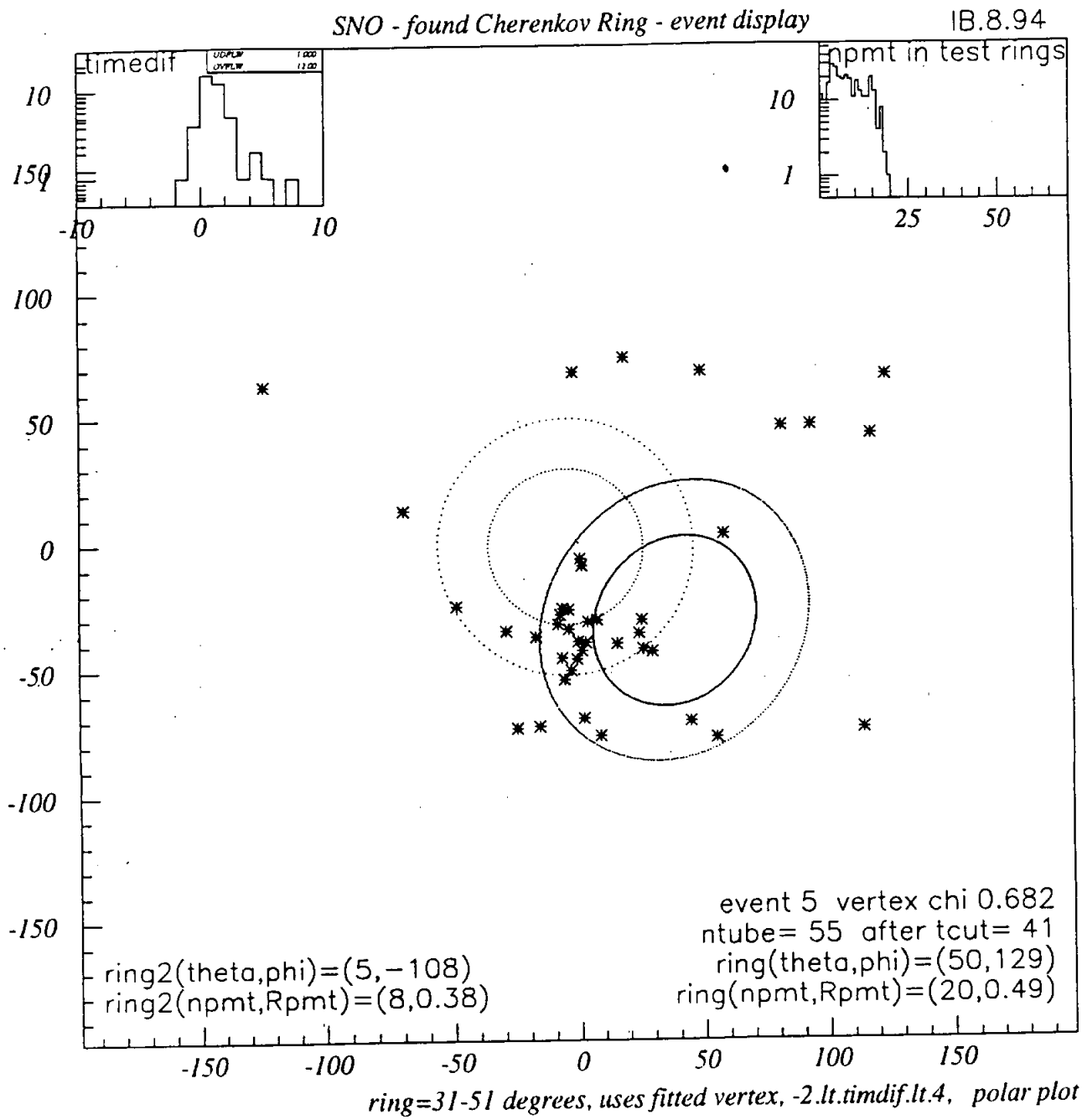
SNO - found Cherenkov Ring - event display
18.8.94
timedif
npmt in test rings
event 5 vertex chi 0.682
ntube= 55 after tcut= 41
ring(theta,phi)=(50,129)
ring(npmt,Rpmt)=(20,0.49)
ring2(theta,phi)=(5,-108)
ring2(npmt,Rpmt)=(8,0.38)
ring=31-51 degrees, uses fitted vertex, -2.lt.timdif.lt.4, polar plot

Fig 9 b

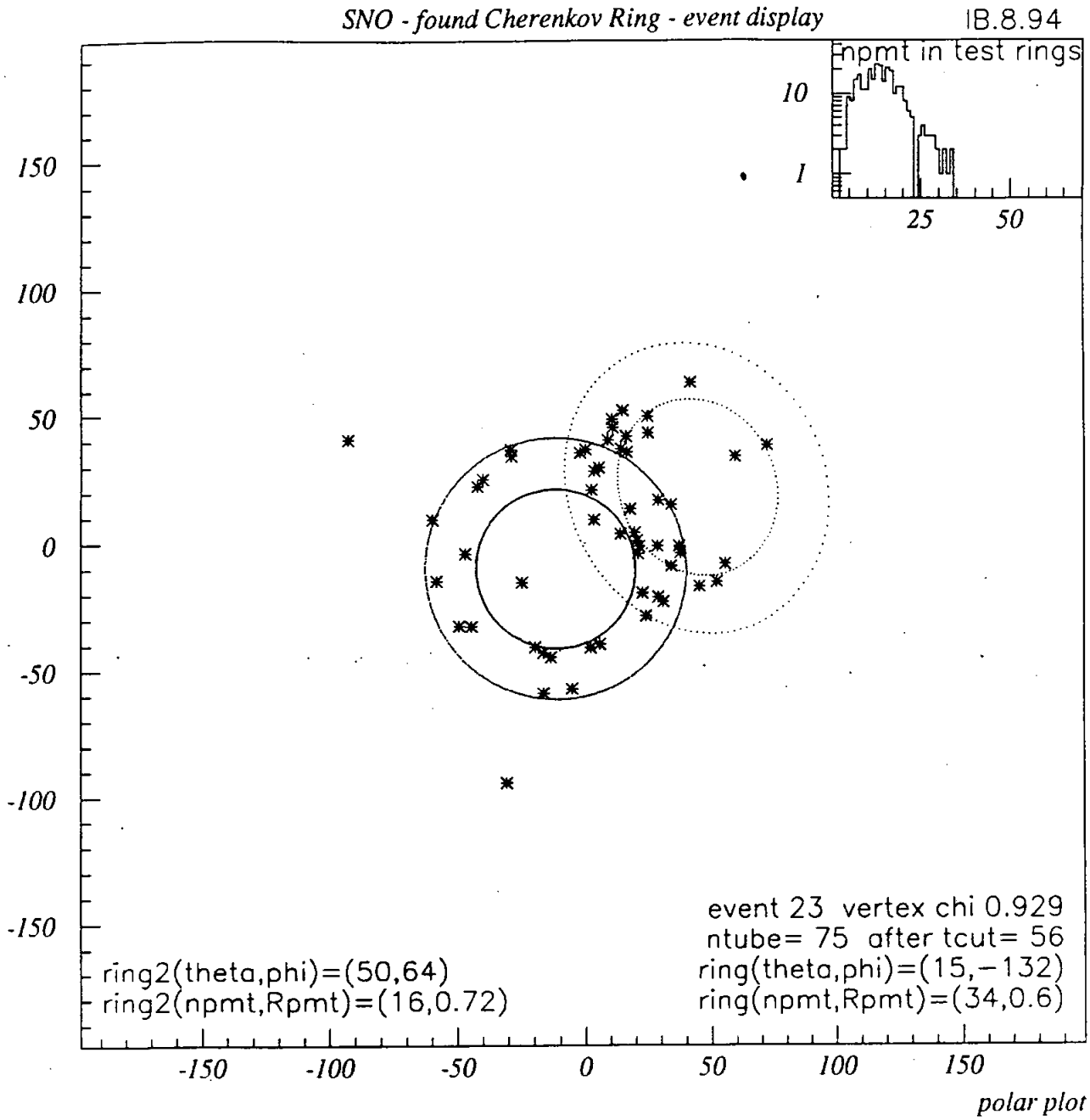
SNO - found Cherenkov Ring - event display
18.8.94
npmt in test rings
10
1
25
50
150
100
50
0
-50
-100
-150
event 23 vertex chi 0.929
ntube= 75 after tcut= 56
ring(theta,phi)=(15,-132)
ring(npmt,Rpmt)=(34,0.6)
ring2(theta,phi)=(50,64)
ring2(npmt,Rpmt)=(16,0.72)
-150
-100
-50
0
50
100
150
polar plot

Fig 9c

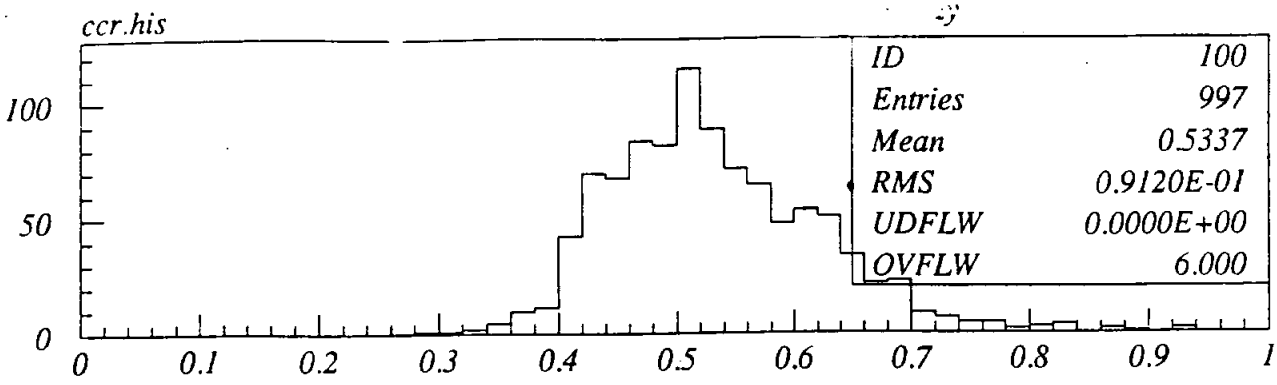

fig 10a

ring1 pmt use

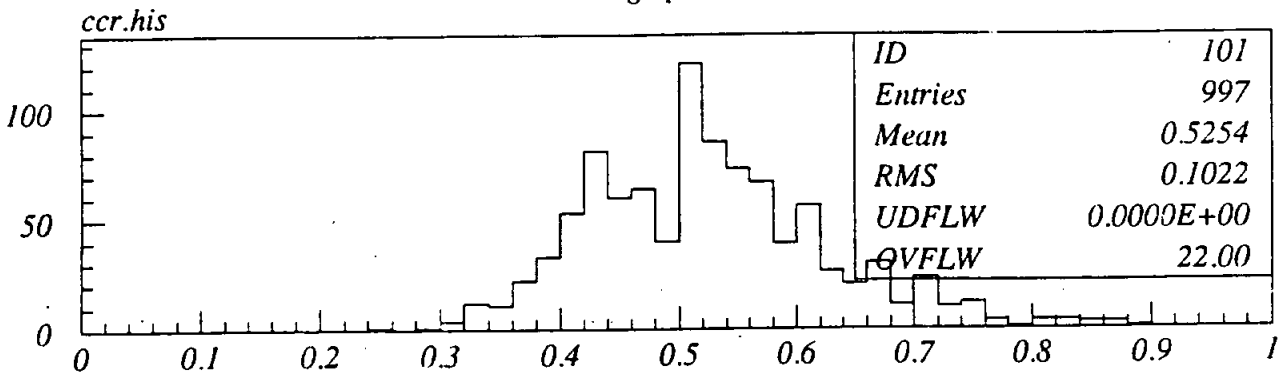

fig 11a

ring2 pmt use

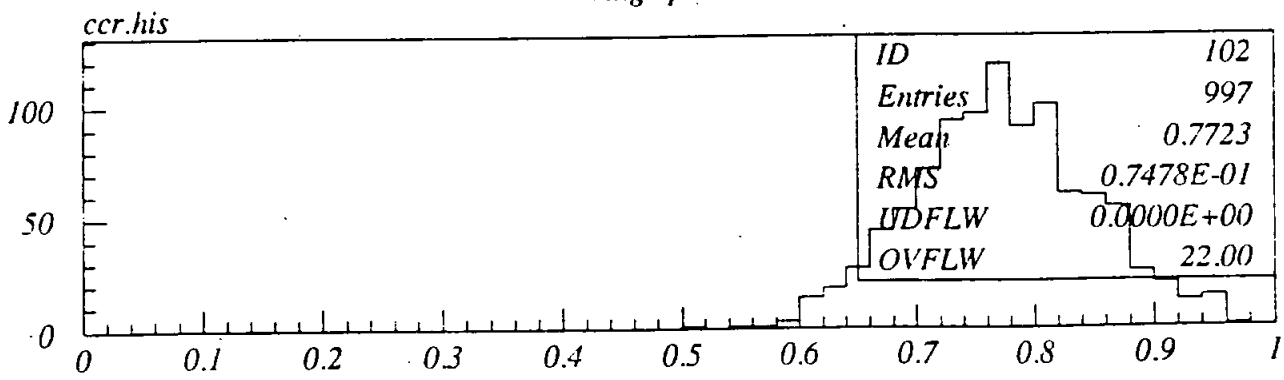

fig 12a

ring1+2 pmt use

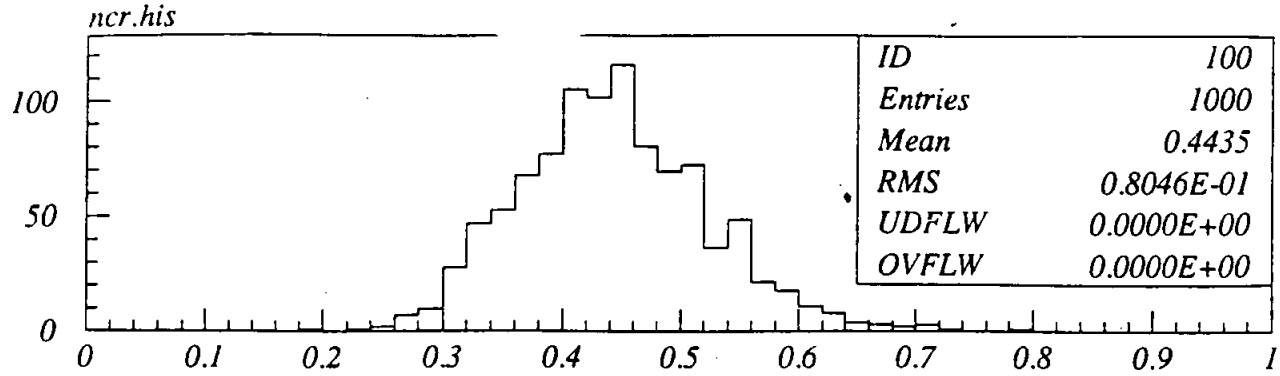

fig 10 b

ring1 pmt use

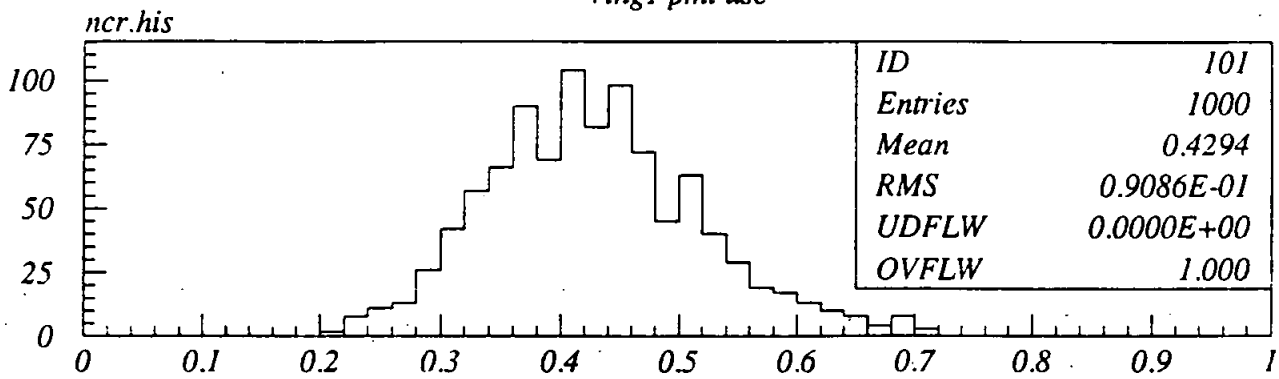

fig 11 b

ring2 pmt use

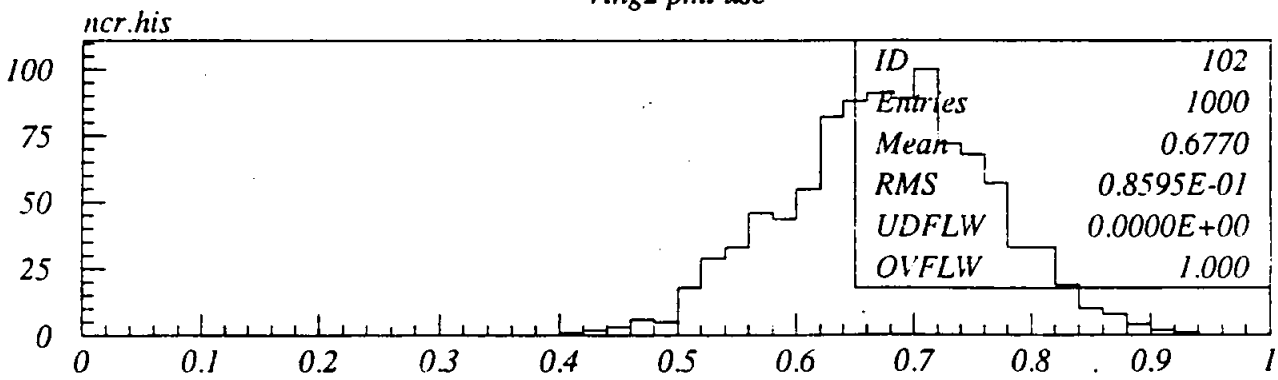

fig 12 b

ring1+2 pmt use

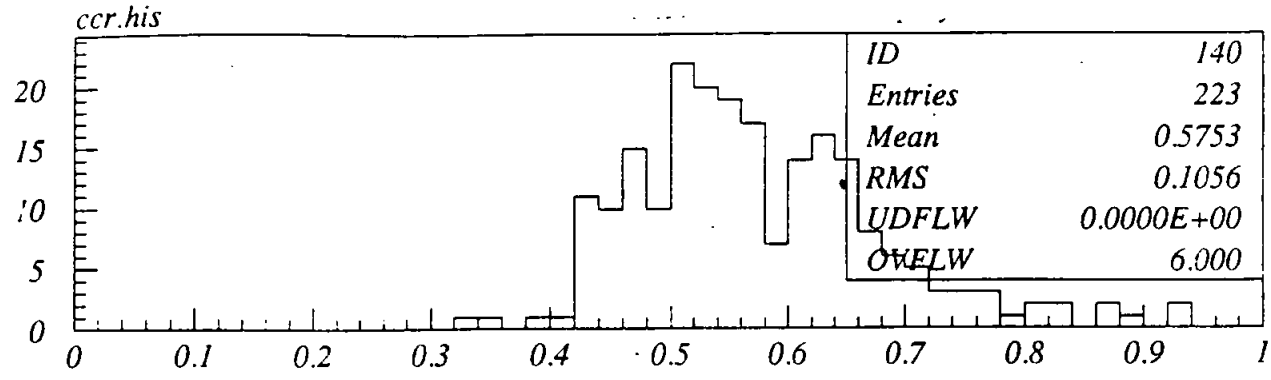

ring1 pmt use

fig 10 c

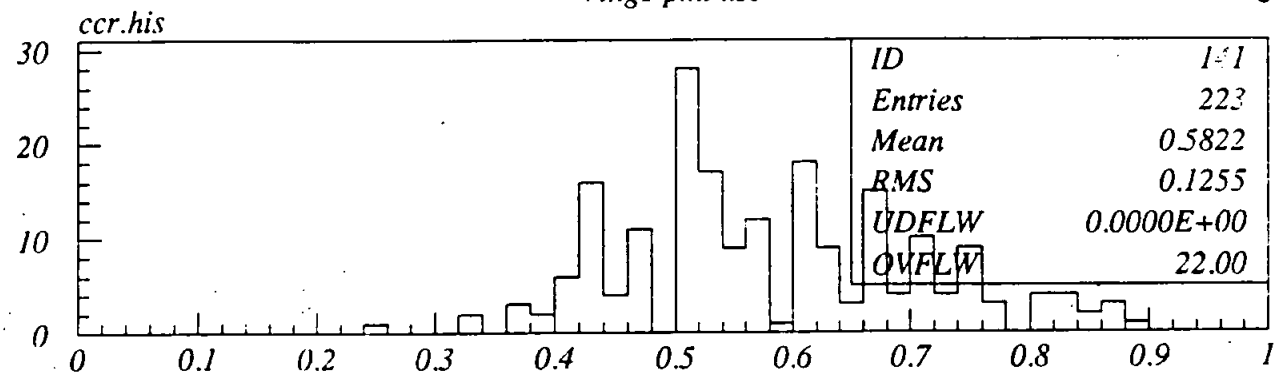

ring2 pmt use

fig 11c

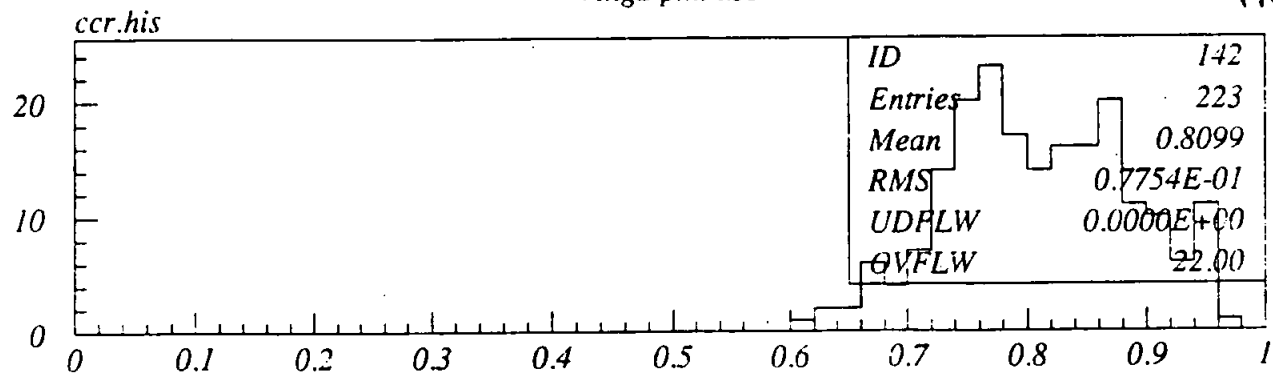

ring1+2 pmt use

fig 12c

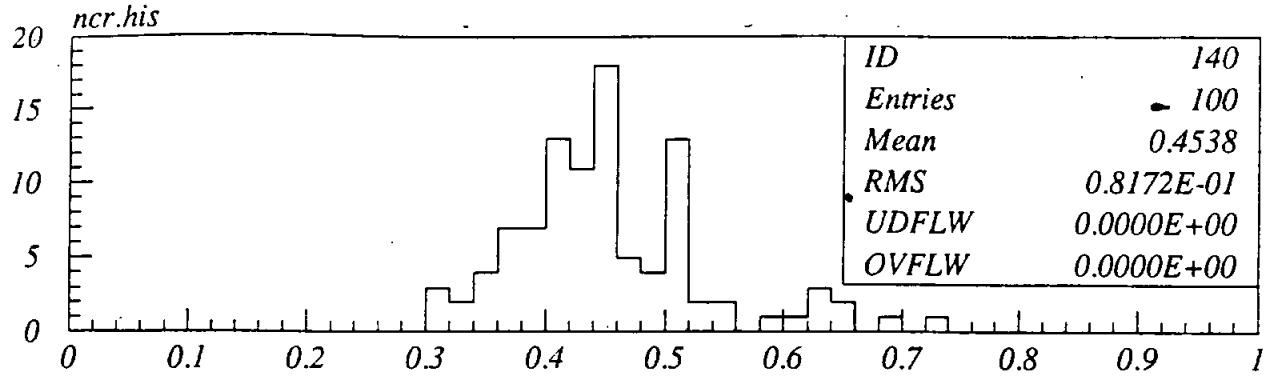

ring1 pmt use

fig 10 d

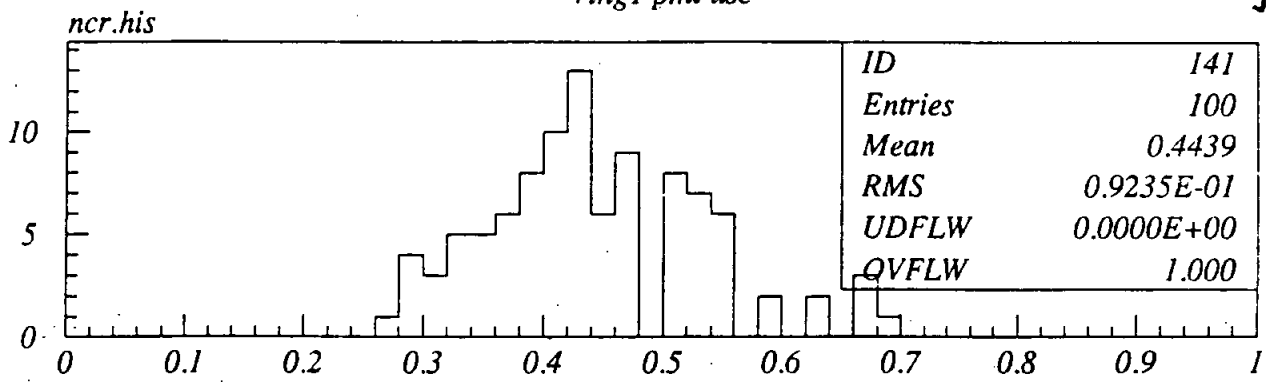

ring2 pmt use

fig 11 d

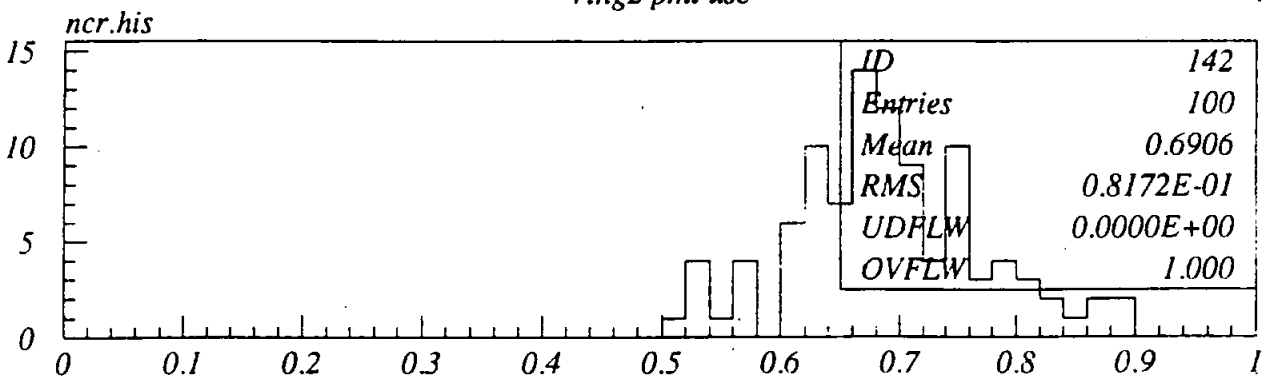

ring1+2 pmt use

fig 12 d

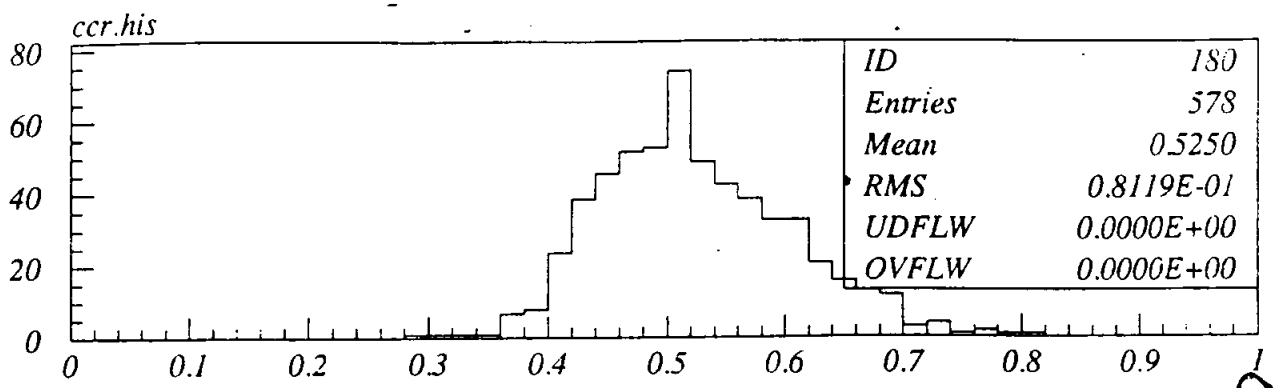

fig 10e

ring1 pmt use

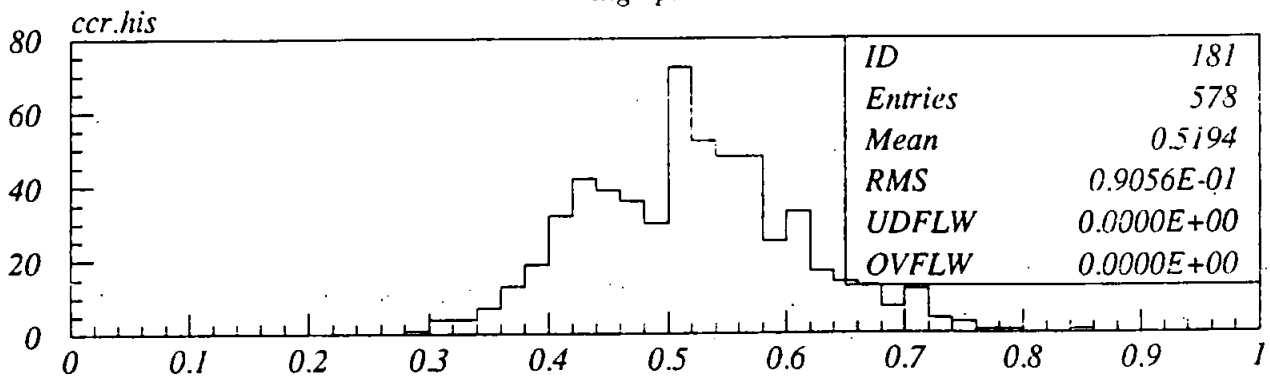

ring2 pmt use

fig 11e

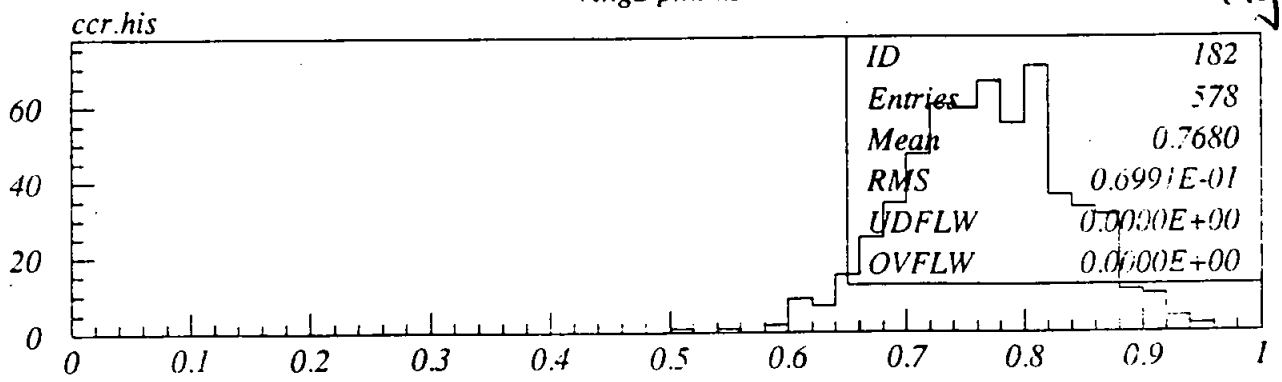

ring1+2 pmt use

fig 12e

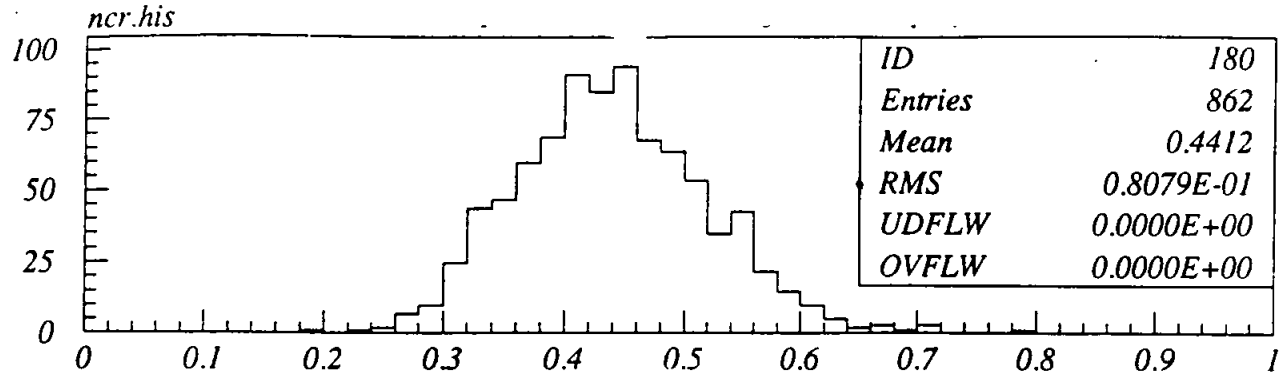

ring1 pmt use

Fig 10f

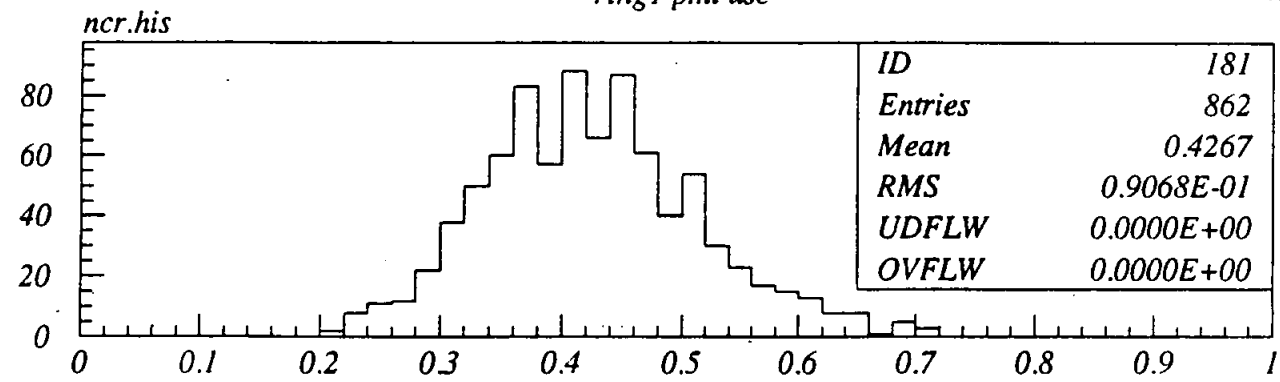

ring2 pmt use

Fig 11f

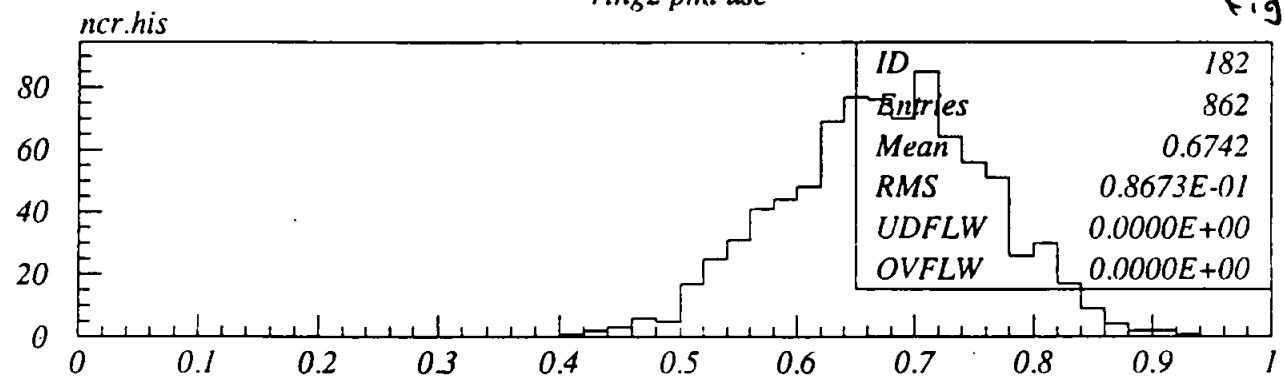

ring1+2 pmt use

fig 12f

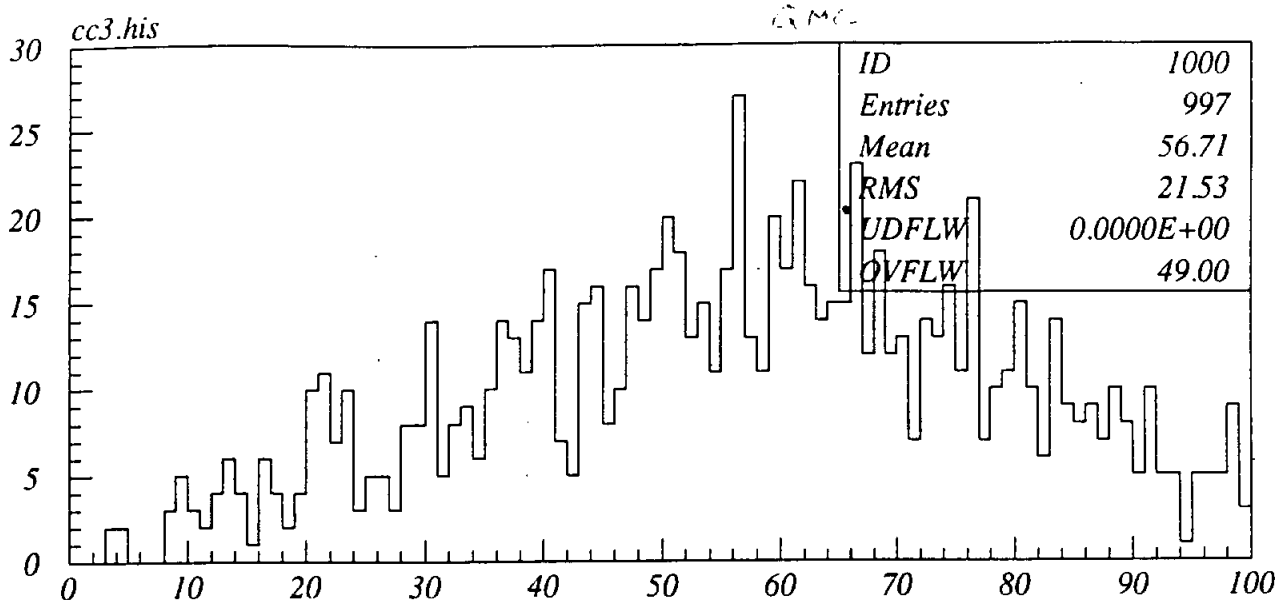
cc3.his
ID 1000
Entries 997
Mean 56.71
RMS 21.53
UDFLW 0.0000E+00
OVFLW 49.00
nhit

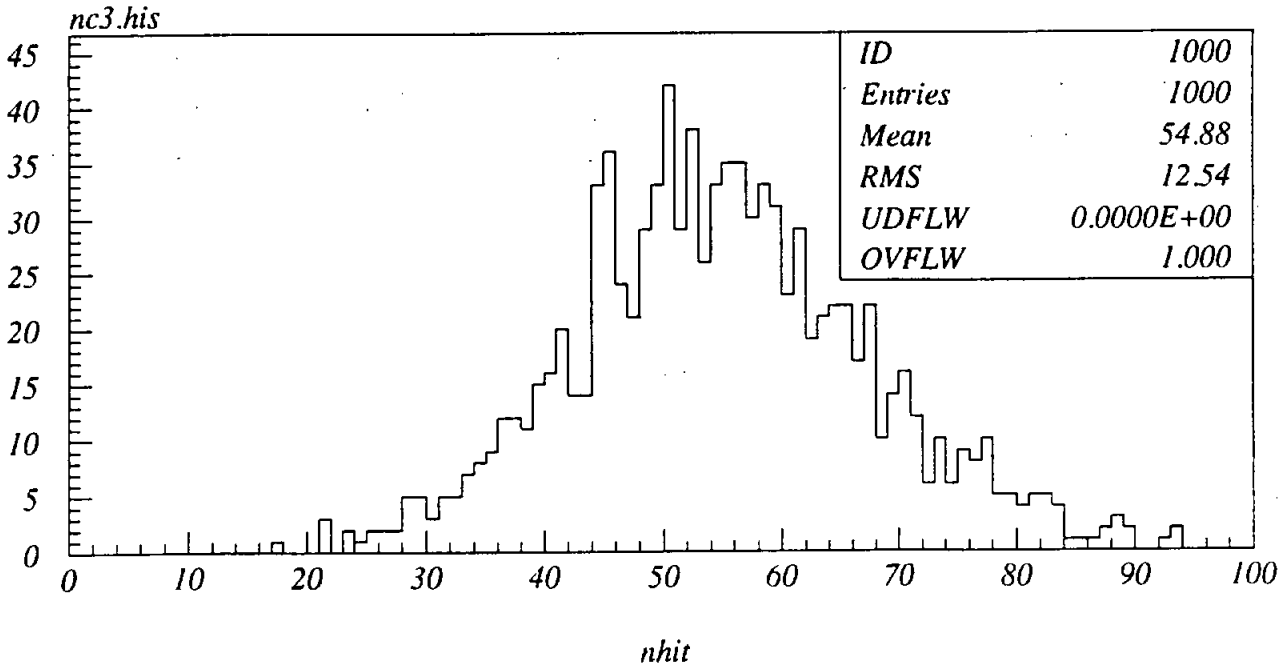
nc3.his
ID 1000
Entries 1000
Mean 54.88
RMS 12.54
UDFLW 0.0000E+00
OVFLW 1.000
nhit

± 4ns Δt cut

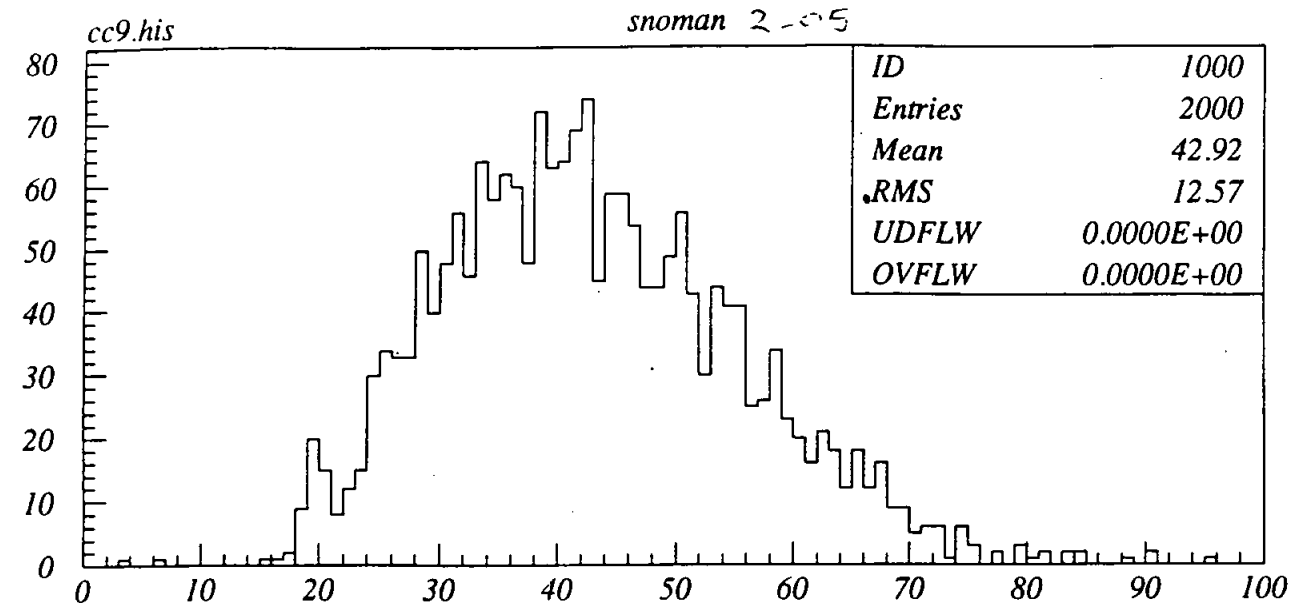

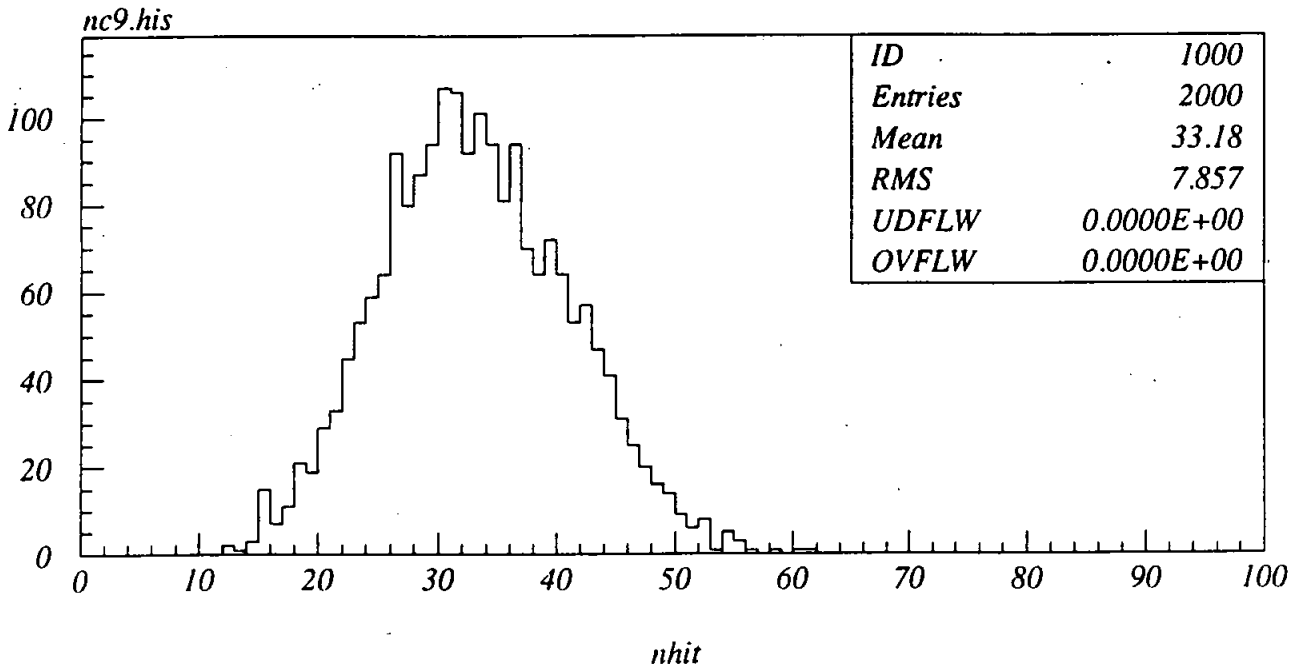

$\pm$ 4ns Δt cut

Fig 13